

Modelling Wave Propagation in the Cochlea

B. Le Henaff, S.J. Elliott and C. Maury

ISVR Technical Memorandum 925

November 2003



SCIENTIFIC PUBLICATIONS BY THE ISVR

Technical Reports are published to promote timely dissemination of research results by ISVR personnel. This medium permits more detailed presentation than is usually acceptable for scientific journals. Responsibility for both the content and any opinions expressed rests entirely with the author(s).

Technical Memoranda are produced to enable the early or preliminary release of information by ISVR personnel where such release is deemed to be appropriate. Information contained in these memoranda may be incomplete, or form part of a continuing programme; this should be borne in mind when using or quoting from these documents.

Contract Reports are produced to record the results of scientific work carried out for sponsors, under contract. The ISVR treats these reports as confidential to sponsors and does not make them available for general circulation. Individual sponsors may, however, authorize subsequent release of the material.

COPYRIGHT NOTICE

(c) ISVR University of Southampton All rights reserved.

ISVR authorises you to view and download the Materials at this Web site ("Site") only for your personal, non-commercial use. This authorization is not a transfer of title in the Materials and copies of the Materials and is subject to the following restrictions: 1) you must retain, on all copies of the Materials downloaded, all copyright and other proprietary notices contained in the Materials; 2) you may not modify the Materials in any way or reproduce or publicly display, perform, or distribute or otherwise use them for any public or commercial purpose; and 3) you must not transfer the Materials to any other person unless you give them notice of, and they agree to accept, the obligations arising under these terms and conditions of use. You agree to abide by all additional restrictions displayed on the Site as it may be updated from time to time. This Site, including all Materials, is protected by worldwide copyright laws and treaty provisions. You agree to comply with all copyright laws worldwide in your use of this Site and to prevent any unauthorised copying of the Materials.

Modelling Wave Propagation in the Cochlea

B Le Henaff, S J Elliott and C Maury

ISVR Technical Memorandum 925

November 2003

UNIVERSITY OF SOUTHAMPTON
INSTITUTE OF SOUND AND VIBRATION RESEARCH
SIGNAL PROCESSING & CONTROL GROUP

Modelling Wave Propagation in the Cochlea

by

B Le Henaff, S J Elliott and C Maury

ISVR Technical Memorandum N° 925

November 2003

Authorised for issue by
Prof S J Elliott
Group Chairman

Acknowledgements

This work of five months (April-August 2003) was made in the frame of my “Travail de Fin d’Etudes” (Final Work of Studentship), it stands for the end of my student life. Through this work, I could also obtain my DEA (Extensive Study Diploma), that allows me to begin a PhD.

This work was made possible thanks to the precious advises of my tutor Steve Elliott, and to Cédric Maury, with whom I shared the office during five months. Also I would like to thank Alison Gunn for her great help and receptiveness during my researches at the library of the ISVR. As well I would like to express gratitude to all the staff of the SPCG, and noticeably Theresa Bravo and Robert Pierzycki for their smile and gladness. Moreover, I am grateful to Marie-Annick Galland, responsible for this work in France at the Centre Acoustique of the Ecole Centrale de Lyon.

Eventually, I would like to salute my flatmates, Andy, Hailey, James, Richard and Paul without whom my stay in Southampton would have been further less enriching for me.

Abstract

The cochlea is the sensory organ of the auditory system, where acoustic signals are converted into nerve impulses, before being conveyed to the brain. Thus, the cochlea achieves a signal processing of the mechanical vibrations caused by the vibrations of the eardrum. Major properties of this system are: a very sharp frequency resolution, the ability to provide energy in order to increase this resolution, and non-linearities, apparently responsible for the local control of vibrations. Several approaches exist for the modelling of these properties, the aim here is to start with a straightforward model (linear, one dimension) and the fundamental physics of the cochlear system in the frequency domain.

We first present the hypothesis and simplifications necessary to make the cochlear system mathematically tractable, in order to implement a passive model and two active models, then further study is made to evaluate the validity of these models. Many investigations exist for the modelling of the active properties of the cochlea, but few of them are completed by a consistent investigation of the cochlear stability. These models are generally made up of a bank of resonators. Considering the active model proposed by Neely and Kim [3], the strategy has been to verify the stability of one of these resonators has been verified when isolated. An approach is proposed here of assessing the stability of the entire model, where interactions between these resonators is considered through the fluid coupling.

Resumé

La cochlée représente l'organe sensoriel du système auditif, elle est le lieu de transduction du signal acoustique en impulsions nerveuses, qui sont par la suite transmises au cerveau. La cochlée réalise donc un traitement du signal vibratoire généré par le tympan. Les propriétés les plus notables de ce système mécanique sont : une discrimination fréquentielle très fine, la capacité à fournir de l'énergie afin d'améliorer encore cette résolution, et des phénomènes non-linéaires qui semblent être responsables d'un contrôle local des vibrations. Plusieurs approches existent pour modéliser ces phénomènes, le but de cette étude est d'abord de réaliser un modèle simple (linéaire, mono-dimensionnel) capable de rendre compte de la physique de base du système cochléaire dans le domaine fréquentiel.

Dans un premier temps, nous présentons les hypothèses et simplifications nécessaires pour rendre le système cochléaire exploitable d'un point de vue mathématique, ceci afin de développer un modèle passif et deux modèles actifs, par la suite une étude plus approfondie est menée pour évaluer la validité de ces modèles. Beaucoup de propositions existent pour modéliser les propriétés actives de la cochlée, mais rares sont les tentatives pour évaluer la stabilité du système. Ces modèles sont constitués d'une série de résonateurs, en considérant le modèle actif proposé par Neely et Kim [3], la stratégie a été de vérifier la stabilité de l'un de ces résonateurs isolé, et ensuite de proposer une approche pour évaluer la stabilité du système complet, pour lequel des interactions de couplages par le fluide sont considérées.

CONTENTS

Page N°

List of symbols	vi
Introduction	1
A. Cochlear physiology and travelling waves	2
A.1. Introduction	2
A.2. Physiology and anatomy of the cochlear system	2
A.2.a. <i>The principal structures of human ear</i>	2
A.2.b. <i>Physiology and anatomy of the cochlea</i>	3
A.2.c. <i>Active mechanics within the cochlear system</i>	4
B. Cochlear models	7
B.1. Basics of cochlear model	7
B.1.a. <i>Introduction</i>	7
B.1.b. <i>Hypothesis for the build of the cochlear model</i>	7
B.1.c. <i>The macromechanical variables</i>	8
B.1.d. <i>Symmetry relations in the upper and lower channels</i>	9
B.2. The long wave model and the 1 D equation	9
B.2.a. <i>Introduction</i>	9
B.2.b. <i>Derivation of the long wave equation</i>	10
B.2.c. <i>Boundary conditions</i>	12
B.2.d. <i>Impedance of the cochlear partition, the passive long wave model</i>	13
B.2.e. <i>Impedance of the cochlear partition, locally active long wave models</i>	17
B.3. Implementation of the cochlear model using the finite difference method	19
B.4. Results of the cochlear models	20
B.4.a. <i>Layout of the results</i>	20
B.4.b. <i>Kanis and de Boer passive models</i>	22
B.4.c. <i>Neely and Kim locally active model</i>	23
B.4.d. <i>Kanis and de Boer locally active model</i>	25
B.5. Network model of the cochlea	26
C. Validity of the models	28
C.1. The long wave criterion	28
C.2. Convergence of the model	29
C.2.a. <i>Analytic evaluation</i>	29
C.2.b. <i>Numerical evaluation</i>	30
C.3. Check of the reciprocity of the model	31
C.3.a. <i>Principle</i>	31
C.3.b. <i>Reciprocity within the fluid</i>	32
C.3.c. <i>Reciprocity within the cochlear partition</i>	33

D. Build of a comprehensive model of the ear	37
D.1. Ear canal and middle ear representations	37
D.1.a. <i>The ear canal model</i>	37
D.1.b. <i>The middle ear model</i>	38
D.2. Check of the reciprocity of the ear canal and middle ear models	40
D.3. Check of the reciprocity of the whole model (ear canal + middle ear + inner ear)	40
D.3.a. <i>Principle</i>	40
D.3.b. <i>Results</i>	42
E. Stability of the lumped component of the Neely and Kim locally active model	43
E.1. Introduction	43
E.2. Description of the micromechanics	44
E.3. Build of the feedback loop system	46
E.4. The Nyquist criterion	48
E.5. Stability of the plant G and controller H	48
E.6. Stability of the feedback loop system	48
F. Stability of the multichannel system	51
F.1. Introduction	51
F.2. Multichannel feedback control system	52
F.3. Method for the study of stability, generalization of the Nyquist criterion	52
F.4. Results	57
G. Conclusions and recommendations for future work	59
H. References	60

LIST OF SYMBOLS

BM : cochlear partition	C, M: coupling and mobility matrices
CP : cochlear partition	P_d : semi-difference pressure array
IHC : inner hair cell	P_a : active pressure array
OHC : outer hair cell	S: source array
RL : reticular lamina	P_{ref}, v_{ref} : pressure and velocity references (resp: Pa, m.s ⁻¹)
TM : tectorial membrane	$p_i, u_{fi}, v_i, Z_i, S_i$: p_d, u_f, v, Z_{cp} and S at the position i
TW : travelling wave	Z_f : acoustic impedance of the fluid (N.s.m ⁻³)
x, y, z : coordinate system	R_h : fluid damping at the helicotrema
H : height of the upper and lower channels (m)	T_{ij} : terms of transfer matrices
W : width of the cochlear partition (m)	q : volume velocity flow (s ⁻¹)
L : length of th cochlea (m)	Q : volume velocity (m ³ .s ⁻¹)
p_f : pressure within the cochlear fluid (Pa)	P_{ec}, Q_{ec} : pressure and volume velocity at the entry of the ear canal
u_f : fluid velocity in the x direction (m.s ⁻¹)	L_{ec}, d, A_{ec} : length diametre and cross sectional area of the ear canal (resp: m, m and m ²)
v_f : fluid velocity in the y direction (m.s ⁻¹)	P_{ed}, Q_{ed} : pressure and volume velocity at the eardrum
u_{st} : velocity of the stapes (oval window) (m.s ⁻¹)	ρ_0 : density of air (kg.m ³)
u_{rw} : velocity of the round window (m.s ⁻¹)	c_0 : speed of sound in the air (m.s ⁻¹)
v : z-velocity of the CP (m.s ⁻¹)	Q_0 : volume velocity of the probe (m ³ .s ⁻¹)
p_d : semi-difference pressure across the CP (Pa)	Y_0 : admittance of the probe (S.I.)
p_a : active pressure (Pa)	A_{st} : area of the stapes (m ²)
Z_{cp} and Y_{cp} : impedance and admittance of CP (N.s.m ⁻³)	ξ_p : average z displacement of CP over width of CP (m)
k_{tw} : wave number of the TW (m.s ⁻¹)	ξ_b : maximum z displacement of CP over width of CP (m)
c_{tw} : phase speed of the TW (m.s ⁻¹)	ξ_c : shear displacement between TM and RL (m)
ω : frequency (rad.s ⁻¹)	ξ_t : component of ξ_c due to TM displacement (m)
Z_{ca} : impedance associated with cochlear amplifier described by Kanis and de Boer (N.s.m ⁻³)	G, H : components of the feedback loop single-channel system
ρ : density of cochlear fluid (kg.m ⁻³)	\mathbf{G}, \mathbf{H} : matrices of the feedback loop multichannel system
α : exponent of the exponential functions	Ξ_b : CP displacement array
m, r, s : mass, damping and stiffness of the CP (resp: kg.m ² , kg.m ⁻² .s ⁻¹ , N.m ⁻³)	$\mathbf{Z}_H, \mathbf{M}_{pass}, \mathbf{B}$: matrices associated with the multichannel system
f_c : characteristic frequency (Hz)	π : 3.14159
g : BM to IHC lever gain	i : index for posititon along cochlea
Z_1, Z_2, Z_3, Z_4 : impedances associated with the micromechanics of the OC (N.s.m ⁻³)	N or N_s : number of spatial points used to represent cochlea in the x-direction
$Z1, Z2, Z3, Z4$: impedances associated with the network model of the middle ear (Kringelbotn)	Δ : thickness of cross-sectional element of cochlea (m)
γ : OHC force generation gain	j : unit imaginary
Z_{pass} : impedance associated with the passive model	

Introduction

The Institute of Sound and Vibration Research (ISVR)

The Institute of Sound and Vibration Research is part of the University of Southampton (UK), it is made up with four main Research Groups. The Dynamics group is in the broad field of vibrational dynamics, including automotive and railway noise and vibration, rotor dynamics vibration of pipes, and smart structures. Particular focus is made on new methods of numerical analysis and especially the “mid-frequency” range. Progress are being made in Statistical Energy Analysis, force determination by inverse method and the active control of structures. The work of Fluid Dynamics and Acoustics Group is focused on aeroacoustics and hydroacoustics. We can mention that applications of techniques based on the numerical solution of the linearised Euler equations are used for the complex flow interactions problem, this group has a strong relationship with Rolls Royce. The Hearing and Balance Centre and the Human Factors Research Unit are concerned by research on audiology and by the development and evaluation of new hearing aid technologies, the interaction between these devices and the process of spatial hearing is also being investigated.

This work has been achieved in the Signal Processing and Control Group (SPCG), in fact this group has expanded to embrace topics in biomedical signal processing (voice modelling, speech enhancement for hearing aids, image processing...). The more established areas of active control of sound and vibration and underwater signal processing remain highly productive themes of work for the SPCG.

Modelling wave propagation in the cochlea

The project is comprises several aims, at first we will present the main characteristics of the cochlea (section A). Then we develop a simple passive, linear and one-dimensional model, in order to understand the basic physics of the cochlear system, this part is completed by two examples of locally active models, able to give the sharp tuning characteristics of the cochlea (section B). Next (section C), we evaluate few numerical and physical characteristics of the models: reciprocity, convergence, respect of the “long wave criterion”. Section D dedicated to the build of a comprehensive model of the ear, completed by a study of the reciprocity of the model created. And finally, Sections E and F deal with an attempt to assess the stability of the locally active model; in a first part we try to evaluate the stability of one component of the cochlea, and then we focus on the stability of the whole model.

A. Cochlear physiology and travelling waves

A.1. Introduction

The fundamental physics of wave propagation along the cochlea is reasonably well understood. The distribution of cochlear fluids in the upper and lower channels of the cochlea, together with the mechanical properties of the basilar membrane, give rise to a dispersive wave, whose velocity falls as it moves along the cochlea. This passive wave propagation is increased by an active cochlear amplification mechanism, involving the inner and outer hair cells, which occurs at each position along the basilar membrane during transduction. However, the active amplification process is considerably less well understood than the passive wave propagation process.

In this section is presented an overview of the anatomy and physiology of cochlea, based on biological surveys and observations. Also we briefly explain the generation of the travelling waves, and the basics of the active process within the cochlea.

A.2. Physiology and anatomy of the auditory system

A.2.a. *The principal structures of human ear*

The ear divides into three main parts, the outer, middle and inner ears (Fig.1). The outer ear is the section to the left of the eardrum in the figure. The main functions of the outer ear are to provide maximal amplitude of the sound wave at the eardrum and to assist with sound location.

The middle ear consists of three ossicles (bones), the malleus, the incus and the stapes. The malleus connects to the eardrum and the stapes to the oval window on the cochlea. The aim of the three bones is to provide a lever arrangement, optimizing energy transfer from the outer ear, which is air filled, to the cochlea which is fluid filled; in a way, middle ear achieve an impedance matching between those two organs.

The inner ear consists of two structures, embedded in the temporal bones, the cochlea and the vestibular organs. The vestibular organ is involved in the sense of balance, it will not be considered here. The cochlea is the sensory organ for the auditory system. It is a coiled bony structure consisting, in humans, of just over two and a half turns. Its uncoiled length is about 3.5 cm.

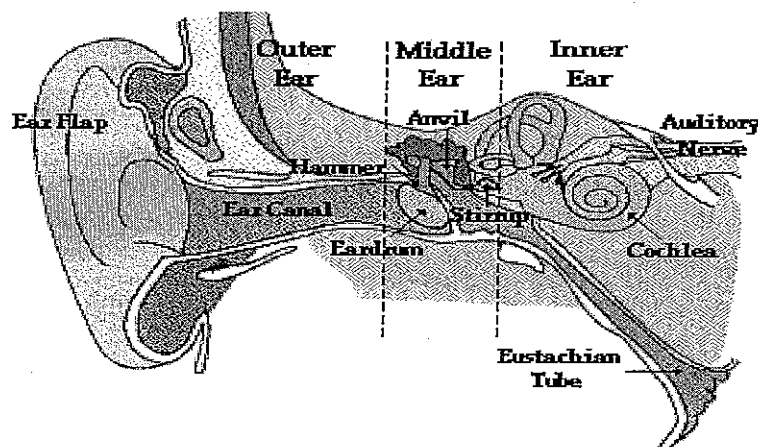


Figure 1: Principal structures of the human ear

A.2.b. Physiology and anatomy of the cochlea

The cochlea (Fig.2a and 2b) is divided in its length into three regions by a pair of membranes (Fig.3). The central region, termed the scala media, is separated from the scala tympani by the basilar membrane (BM) and from the scala vestibuli by Reissner's membrane. The scala media is filled with endolymph, whose mechanical properties are similar to water; organ of Corti is enclosed in this scala media, and supported by the BM. The scala media narrows toward the apical end of the cochlea. Scala vestibuli and scala tympani are filled with perilymph, it differs from endolymph with its ionic composition; a small opening called helicotrema connects those two scalae at the apical end of cochlea. Fig.3 is a cross section through the cochlea showing the three scalae and these two membranes, along with the organ of Corti, which contains the sensory hair cells and the tectorial membrane noticeably. Moreover, the BM becomes broader, and mechanically more compliant from base to apex, whereas the cross section of the scala media taper in the opposite direction to the BM, becoming narrower from base to apex.

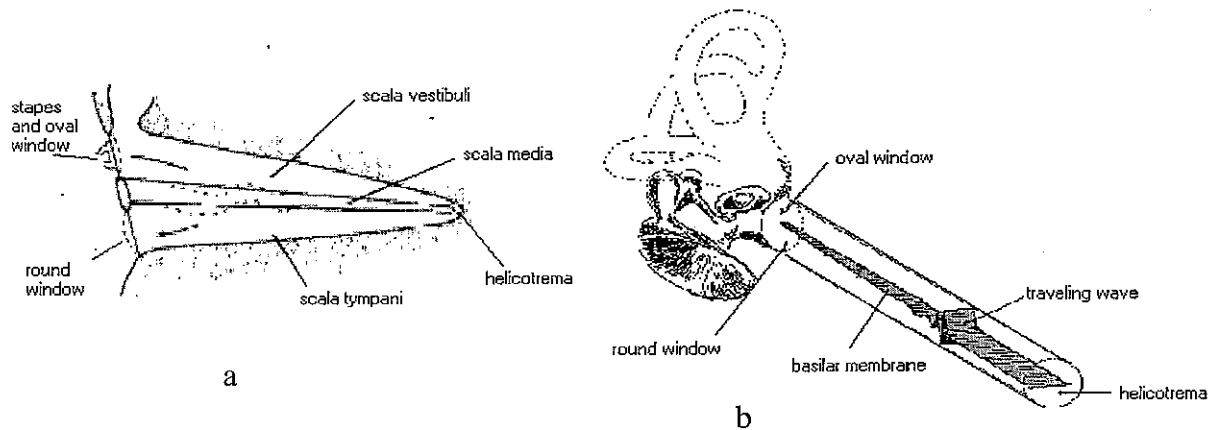


Figure 2: (a and b) Two representations of straightened cochlea

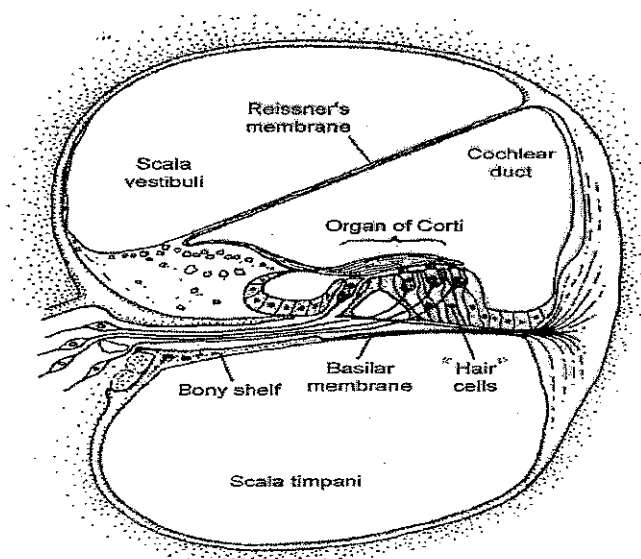


Figure 3: Transversal view of cochlea

Vibrations at the eardrum, generated by acoustic stimuli in the ear canal, are received by the ossicular chain of the middle ear; these motions are then transmitted to the stapes footplate, connected with the oval window, and finally the oval window transfers its motion to the perilymph in scala vestibuli. This duct is on both sides separated from the rest by membranes: the oval and round windows, the round window facing the air filled middle-ear cavity.

Vibrations of the oval window generate a hydromechanical wave involving transverse motion of the BM, which is a part of cochlear partition. The wave, known as the travelling wave (see Fig.4), travels along the BM carrying energy from base to apex. This passive travelling wave propagation involves transfer of mechanical energy between a spatially distributed store of kinetic energy -cochlear fluids- and a spatially distributed store of potential energy -the BM stiffness-. One major observation is that, for a pure tone stimulus, the travelling wave amplitude response varies with position along the BM, peaking at a point which is dependent on the stimulus frequency (characteristic point). The location of the peak in the response gets closer to the base as the frequency increases; hence, to some extent, BM can be seen as a Fourier analyser, which translates frequency into position. This phenomenon is sometimes called spatial nonuniformity; it can be interpreted in terms of wave speed, which varies with position along the cochlea. Moreover, cochlea is a dispersive field since the wave speed also varies with frequency. As we shall see later, those two major facts are due to mechanical properties of the BM.

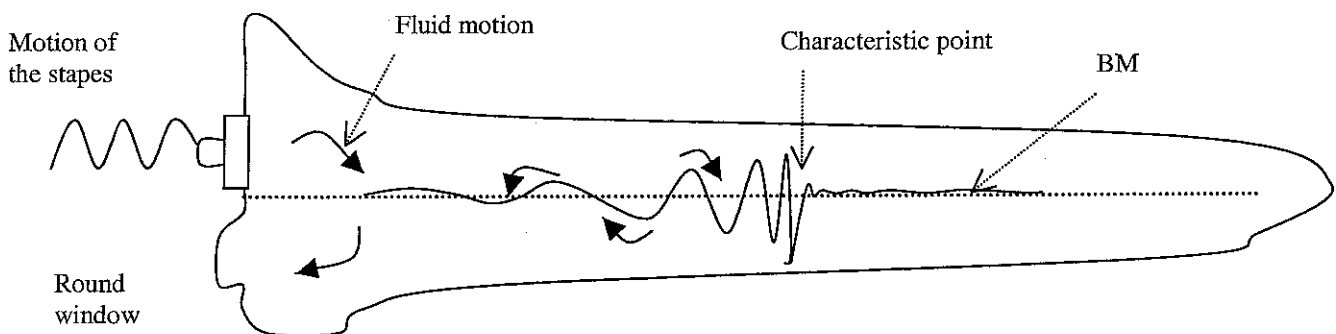


Figure 4: Travelling waves on the basilar membrane

A.2.c Active mechanics within the cochlear system

Organ of Corti mechanics, micromechanics

Mechanics of the organ of Corti are also called micromechanics of the cochlea, that refers to the movement and interaction of the structures attached to the basilar membrane.

The basilar membrane supports a rigid structure formed by the walls of the Corti tunnel (Pillar cells) and the reticular lamina. The inner hair cells and the outer hair cells (IHCs and OHCs) lie under the reticular lamina, the tectorial membrane is a gelatinous structure above the reticular lamina, which is attached at its inner edge and runs along the length of the cochlea. Tectorial membrane and reticular lamina are separated by a layer of endolymph fluid. A bundle of hairs, from both IHCs and OHCs, called stereocilia projects from the top of each hair cell towards the tectorial membrane. The tectorial membrane is

attached to the tallest stereocilia of the outer hair cells (as shown in Fig.5). Deiters' cells provide visco-elastic coupling between the OHCs and the elastic basilar membrane.

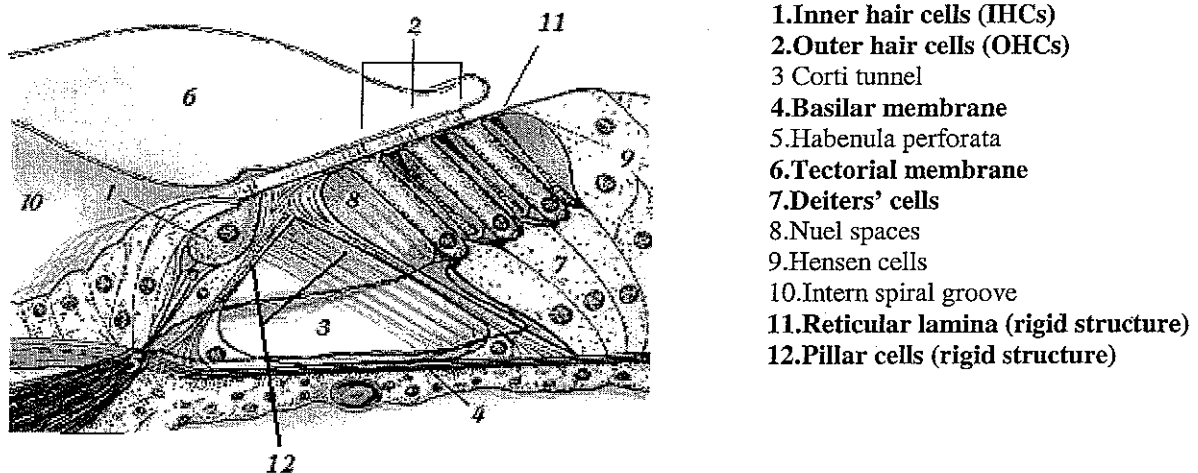


Figure 5:The organ of Corti

OHCs and IHCs added to tectorial membrane (Fig.5) have a key role in the transduction process achieved by the BM. Both types of hair cell convert the displacement of their stereocilia, caused by the relative motion of the reticular lamina and the tectorial membrane, into transducer current that produces a modulation of the cells receptor potential, this is generated by the modification of the rate of flow of ions from the surrounding endolymph to the hair cells. It has been shown that IHCs are the sensory cells of the cochlea given that their synapse is directly connected to the auditory nerve. OHCs are motile, and it is commonly assumed that they can convert membrane potential into a force. The transduction process from mechanical excitation to nerve impulses conveyed to the brain can be summed up by the diagram of Fig.6 :

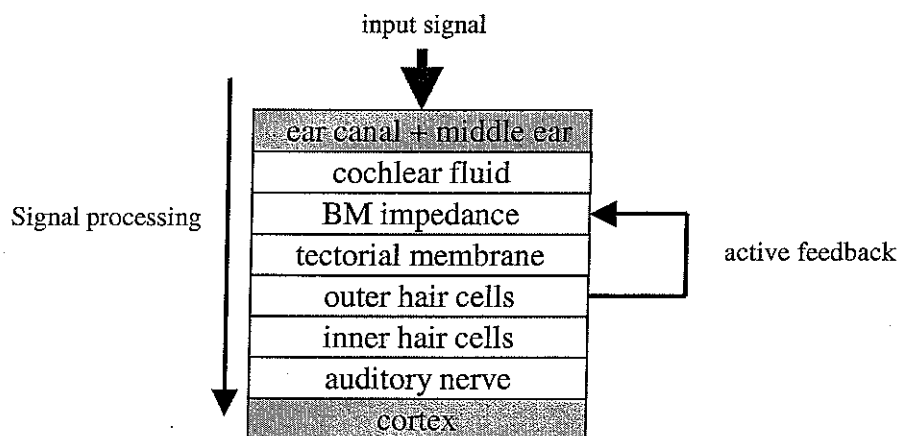


Figure 6: Block diagram of the transduction process within the inner ear

The motion of the cochlear fluid triggers a travelling wave, relative displacement between the basilar membrane and the tectorial membrane provoke the OHCs contraction, hair cells contraction distorts the organ of Corti, the cell length change forces the rigid arch structure formed by the Pillar cells to pivot around the inner attachment of the basilar membrane (Fig.7), so that the motion of the basilar membrane is modified, here emerges the

active mechanical feedback provided by the OHCs. This feedback control seems to guarantee optimal functioning of the cochlear system; it provides both cochlear amplification and saturation properties to the global system.

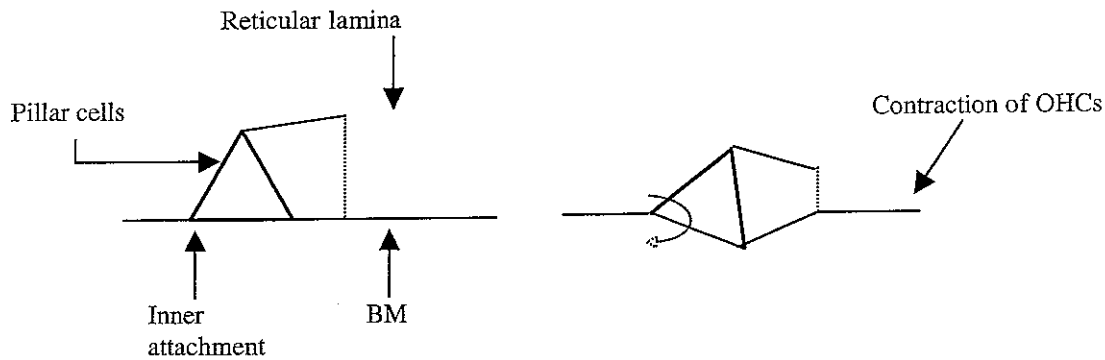


Figure 7: Distortion of the Organ of Corti

Non-linearities

One of the major characteristics of the cochlear system is its non-linearity, experiments on live cochlea have exhibited several non-linear phenomena, mainly due to the OHCs. One of these phenomena is the saturation of the basilar membrane velocity at some input levels. If we display the input-output diagram of the basilar membrane for a fixed frequency (where the input is the pressure imposed at the entry of the ear canal, and the output is the velocity of the basilar membrane) we obtain, basically, the diagram of Fig.8:

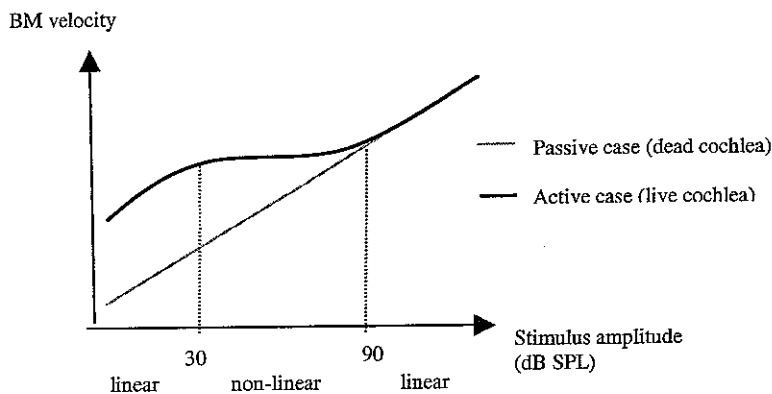


Figure 8: Compressive non-linearity in the basilar membrane response

The basilar membrane motion at low input levels (below 20 dB SPL) is linear but greatly enhanced, compared with the passive case. Between 30 and 90 dB SPL the response saturates, a compressive non-linearity is produced, this phenomena is most often assumed to be due to the active undamping actions provided by the OHCs, this non-linear mechanism is likely to process a local control of vibrations. This action becomes negligible above 90 dB SPL, where the response approaches the linear passive case. This compressive non-linearity generate harmonic distortions, known as the acoustical distortion product. In this document non-linear phenomena will not be considered, consequently we can say that our study is limited to low and high level stimuli (below 30 dB SPL, and above 90 dB SPL). For more justifications, see Nobili et al.[13].

B. Cochlear models

B.1. Basics of the cochlear models

B.1.a. Introduction

The principles explained above have been applied to the implementation of a model in the frequency domain. First, we will present the framework taken for this initial work in particular the hypothesis underlying the basic equations. Then the derivation of the travelling wave equation will be detailed; it will be followed by a presentation of the results obtained using the different models (passive and active). The first aim of this study is to implement a simple passive model of the cochlea, in order to understand the basic phenomena of wave propagation, this first model will be based on the approach developed by de Boer [1], and on Kanis and de Boer [2].

The objective here is to implement a one-dimensional linear model able to capture the main features of cochlear macromechanics in the frequency domain. The basics of the models are mainly quoted from papers by Boer [1], Neely and Kim.[3] and Kanis and de Boer.[2].

B.1.b. Hypothesis for the build of the cochlear models

We have particularly followed the approach used in [1], in which the basics for a one-dimensional, passive and linear model are presented. This work allowed the problem to be made 'mathematically tractable', by proposing the following steps of simplification:

- Cochlea is taken to be straight and with a constant cross-section, instead of coiled and tapered structure.
- The wavelength in the cochlea is assumed to be larger than the dimensions of the cross-section (long-wave approximation).
- Reissner's membrane is ignored, thus the scala vestibuli and scala media are treated as a single fluid channel, called here the upper channel. Scala tympani will be called the lower channel.
- A section across the upper channel (perpendicular to the longitudinal axis) will be considered as rectangular.
- Lower channel is assumed to have the same cross section as the upper channel.
- The BM, the tectorial membrane, the organ of Corti and associated cells are all replaced by a single flexible membrane called the cochlear partition (CP).
- The CP is assumed to be incompressible, it deflects but its volume keeps constant. Consequently, the fluid velocities above and below the CP are equal at any location.
- The stapes footplate stands for the basal boundary of the upper channel, it is perpendicular to the longitudinal axis.
- Helicotrema is modelled as a gap in the CP at the apical end of cochlea, and stands for a fluid connection between the two channels.
- Cochlear fluids (which can be assimilated to water) are assumed incompressible and inviscid (the viscosities and thermal conductivity are zero).

Consequently, the simplified structure of the cochlea will be modelled as follows, that represents the starting point for the macromechanical models (Fig.9)

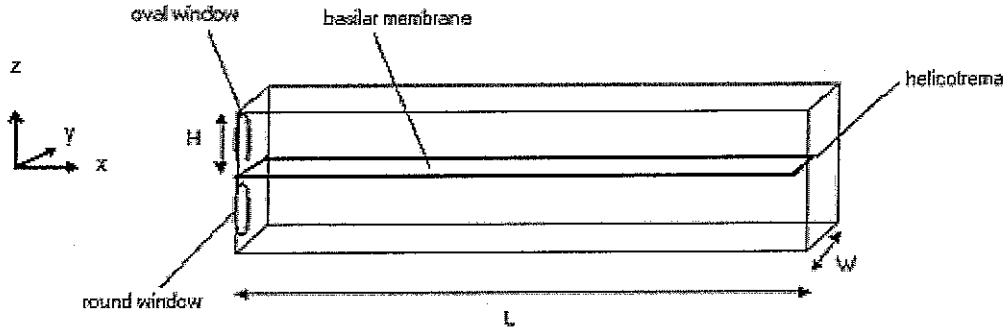


Figure 9: Simplified structure of the cochlea

According to de Boer [1] and Viergever [9], points on the membrane at different longitudinal positions are assumed to have no direct mechanical coupling; all coupling are assumed to occur via the cochlear fluid; this implies that the mechanics of the membrane can be described by a mechanical impedance. The simplest model of this impedance is of a mass-spring damper system at each point along the membrane, with a distribution of those parameters along the cochlea.

As an alternative to this passive long-wave model, we will also test two locally active models proposed by Neely and Kim [3] and Kanis and de Boer.[2]. These models use exactly the same macromechanical framework as the previous one, but introduces micromechanical active elements within the cochlear partition impedance. The interest of these models is that micromechanical effects are characterized as relationships between macromechanical quantities.

B.1.c. The macromechanical variables

For a given sound stimulus, the solution of the macromechanical response is specified in terms of the fluid pressure and the fluid velocity vector at all points and at all instants in time. Once those fluid variables have been determined, the CP velocity and pressure are also known, because the CP is in contact with the fluid. Variables here are specified with reference to the three-dimensional coordinate system shown in Fig.9. In this model, we will not consider lateral variations (along the y axis). At a given point in space and an instant in time, velocity and pressure fields are denoted by:

The fluid pressure: $p_f(x, z, t)$ (Nm^{-2})

The fluid x-velocity vector: $u_f(x, z, t)$ (ms^{-1})

The fluid z-velocity vector: $v_f(x, z, t)$ (ms^{-1})

The velocities at the fluid boundaries are denoted by:

The stapes (oval window) x-velocity: $u_{st}(z, t)$ (ms^{-1})

The round window x-velocity: $u_{rw}(z, t)$ (ms^{-1})

The cochlear partition z-velocity: $v(x, t)$ (ms^{-1})

B.1.d. Symmetry relations in the upper and lower channels

As mentioned by several authors, it is more suitable to consider the semi-difference pressure between upper and lower channel:

$$p_d(x, z, t) = \frac{1}{2}[p_f(x, z, t) - p_f(x, -z, t)] \quad 0 < z < H \quad (\text{B.1})$$

This definition is convenient because, only the semi-difference pressure plays a part in travelling wave propagation (this is demonstrated in Lineton [4]). Indeed, assuming linearity, any arbitrary boundary conditions at the round window and stapes footplate can be split into “push-push” case (application of identical forces to stapes and round window) and “push-pull” case (application of equal and opposite forces to stapes and round window). The “push-push” case activate fast waves (compression waves) to travel up the two cochlear channels, and by symmetry there is no CP displacement and consequently no TW. The “push-pull” case brings about a pressure difference in the two channels thereby generating TW which propagates by CP deflection and also fast waves in the two channels. Given the commonly assumed incompressibility of cochlear fluids, the fast waves can be ignored entirely, thus, in the following parts the perilymph is pushed-pulled by the motion of the oval window and the cochlear duct behaves like fluid column; the round window membrane is moving in opposite direction related to the motion of the oval window membrane. Moreover, in this “push-pull” case, the pressure and velocity at apical locations remain completely unchanged until the arrival of the TW.

Consequently, in our model, velocity and pressure components exhibit the following antisymmetry, t stands for the time:

$$\begin{aligned} u_{rv}(-z, t) &= -u_{st}(z, t) \\ u_f(x, -z, t) &= -u_f(x, z, t) \\ v_f(x, -z, t) &= v_f(x, z, t) \\ p_f(x, z, t) &= -p_f(x, -z, t) \end{aligned} \quad (\text{B.2})$$

According to this last relation we have:

$$p_d(x, z, t) = p_f(x, z, t) \quad (\text{B.3})$$

B.2. The long-wave model and the 1-D equation

B.2.a. Introduction

Given the assumptions made in the previous section, we can now introduce the equations governing travelling wave propagation. The semi-difference pressure in the cochlear fluid can be now related to the motions of the stapes footplate, using the equations of fluid mechanics and the impedance of the CP. Fluid viscosity is ignored, since the system is damped via the resistive component of the CP impedance. Particles displacements and velocities are considered very small compared to characteristic dimensions of the model and wave speed respectively. As we already mentioned, the cochlear fluid is assumed inviscid

incompressible (ρ is constant). The following calculation is inspired by Lineton [4]. The analysis yields partial differential equations for the fluid flow (pressure and velocity), in which both the axial and transverse dimensions appear as independent variables. Using the “long-wave approximation”, we can eliminate the transverse coordinate as an independent variable. Thus, as we will see, the mechanics of the long wave model can be represented as a simple one-dimensional wave equation.

B.2.b.Derivation of the long wave equation

As mentioned above, the fluid pressures in the two channels are antisymmetric, thus the fluid pressure in the upper channel is equal to the semi-difference pressure p_d .

First, cochlear fluid in the upper channel obeys the conservation of mass ($\text{div}(\vec{v}_{\text{fluid}}) = 0$):

$$\frac{\partial u_f(x, z, t)}{\partial x} + \frac{\partial v_f(x, z, t)}{\partial z} = 0, \quad (\text{B.4})$$

and the equations of conservation of momentum in two directions:

$$\frac{\partial p_d(x, z, t)}{\partial x} = -\rho \frac{\partial u_f(x, z, t)}{\partial t}, \quad (x \text{ direction}) \quad (\text{B.5})$$

$$\frac{\partial p_d(x, z, t)}{\partial z} = -\rho \frac{\partial v_f(x, z, t)}{\partial t}. \quad (z \text{ direction}) \quad (\text{B.6})$$

We also have the boundary conditions at the stapes footplate and at the helicotrema, the stapes x -velocity being assumed independent of z :

$$\begin{aligned} u_f(0, z, t) &= u_{st}(t), \\ u_f(L, z, t) &= 0, \end{aligned} \quad (\forall z, t) \quad (\text{B.7})$$

and the boundary conditions at the CP and ceiling of the upper channel:

$$\begin{aligned} v_f(x, 0, t) &= v(x, t), \\ u_f(x, H, t) &= 0. \end{aligned} \quad (\forall x, t) \quad (\text{B.8})$$

Then, in the long wave approximation, it is assumed that the z -velocity of the fluid varies linearly across the cochlea:

$$v_f(x, z, t) = \left(1 - \frac{z}{H}\right)v(x, t). \quad (\text{B.9})$$

Using this equation does not violate the conservation of the z -momentum provided that: $v_f(x, z, t) \ll u_f(x, z, t)$. This condition is satisfied as long as H is much smaller than the wavelength of the travelling wave. Differentiating (B.9) with respect to z , and substituting into (B.4), we obtain:

$$\frac{\partial u_f(x, z, t)}{\partial x} = \frac{v(x, t)}{H}. \quad (\text{B.10})$$

The right-hand side of (B.10) is independent on z , so is the left side. Equation (B.10) and assumption that stapes footplate velocity is independent of z allow us to say that $u(x, z, t)$ is independent of z . Also, from (B.5), the pressure becomes independent of z . It follows that both fluid pressure and x -velocity are uniform across the upper channel; consequently, the z variable can be dropped from the equations.

Differentiating (B.10) with respect to t , and (B.5) with respect to x we can equal terms to give:

$$\frac{\partial^2 p_d(x, t)}{\partial x^2} = -\rho \frac{\partial^2 u_f(x, t)}{\partial x \partial t} = -\frac{\rho}{H} \frac{\partial v(x, t)}{\partial t}. \quad (\text{B.11})$$

Transforming (B.11) into the frequency domain gives (ω being the radian frequency) and assuming a harmonic time dependence in $e^{+j\omega t}$ for v :

$$\frac{\partial^2 p_d(x, \omega)}{\partial x^2} = -j \frac{\omega \rho}{H} v(x, \omega) \quad (\text{B.12})$$

Introduction of CP impedance

To introduce this impedance, we can use an electronic analogy, considering CP as a passive receptor, which undergoes the current intensity v , and the tension $-2p_d$.

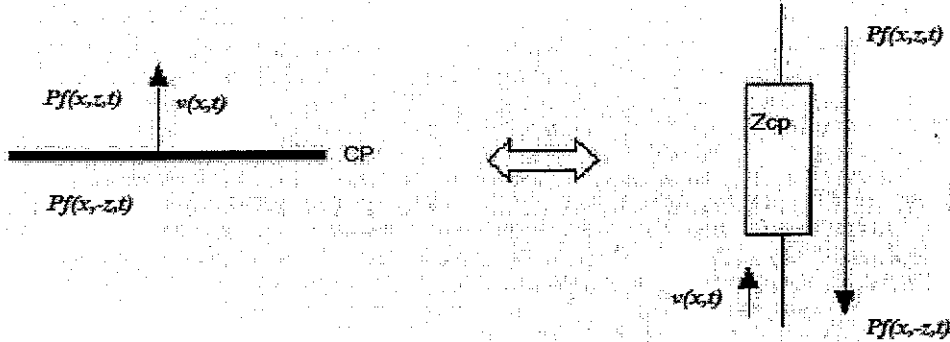


Figure 10: Electronic analogy

Following the right-hand side of Fig.10:

$$p_f(x, -z, t) - p_f(x, z, t) = Z_{cp} \cdot v(x, t). \quad (\text{B.13})$$

Consequently the impedance of this receptor is, in the frequency domain:

$$Z_{cp}(x, \omega) = \frac{-2p_d}{v}. \quad (\text{B.14})$$

all those variables depending on x and ω .

Combining (B.12) and (B.14) we obtain:

$$\frac{\partial^2 p_d(x, \omega)}{\partial x^2} - \frac{2j\omega\rho}{HZ_{cp}(x, \omega)} p_d(x, \omega) = 0 \quad (\text{B.15})$$

Rearranging equation (B.15), we obtain the wave equation:

$$\frac{\partial^2 p_d(x, \omega)}{\partial x^2} + k_{TW}^2(x, \omega) p_d(x, \omega) = 0, \quad (\text{B.16})$$

with:

$$k_{TW}(x, \omega) = \frac{\omega}{c_{TW}(x, \omega)} \quad (\text{B.17})$$

where

$$c_{TW}^2(x, \omega) = \frac{j\omega HZ_{cp}(x, \omega)}{2\rho} \quad (\text{B.18})$$

Where k_{TW} and c_{TW} are the wave number and the phase speed of the travelling wave respectively.

Note that equation (B.16) can be considered as a 1-D Helmholtz equation, it differs from the 'classic' version, since it is distributed and dispersive with its wave number is dependent both on x and ω .

B.2.c Boundary conditions

In order to close the system, we have to define the boundary conditions:

At the base

if we apply the x -momentum equation at $x=0$, and assuming that the stapes footplate velocity (u_{st}) is known, we obtain:

$$\frac{dp_d(0)}{dx} = -j2\omega\rho u_{st}, \quad (\text{B.19})$$

The stapes footplate is then considered as a rigid boundary.

At the apex

A commonly used boundary condition at the helicotrema is:

$$p_d(L) = 0. \quad (\text{B.20})$$

This is physically justified if we consider the helicotrema as a fluid connexion between the two channels, consequently the semi-difference pressure is logically equal to zero. Several authors propose another boundary condition taking into account the fluid damping at the helicotrema. According to [4], the justification for equation (B.20) is also that the model response is highly insensitive to this apical boundary condition, provided

the stimulus frequency is high enough to ensure that the characteristic place lies basal to the helicotrema.

B.2.d Impedance of CP, the passive long wave model

The main differences between the various 1-D models of cochlea lie in the assumed impedance of the cochlear partition Z_{cp} . The formulation adopted here is taken from de Boer [1] and Kanis and de Boer [2].

(N.B.: In those documents the value for H (height of the upper channel) is : 0.001 m)

The passive impedance is given as follows:

$$Z_{cp}(x) = j\omega m(x) + r(x) + s(x)/j\omega. \quad (B.21)$$

It is made up with a mass term (positive imaginary), a resistive term, (positive in the passive model), and a stiffness component (negative imaginary). This formulation of impedance is both dependent on ω and x .

If we continue to follow de Boer's approach, we can adopt the following expressions for impedance components:

- the stiffness component is assumed to decrease with increasing x as an exponential function: $s(x) = s_0 e^{(-\alpha x)} (N.m^{-3})$. This assumption is based on experimental evidence.
- The mass component is assumed to be constant along the cochlea: $m_0 (kg.m^{-2})$
- The resistance is taken as an exponential function: $r_0 e^{(-\alpha x/2)} (N.s.m^{-3})$

These distributions are illustrated in Fig.11

Thus, the impedance can be written as:

$$Z_{cp}(x, \omega) = j\omega m_0 + r_0 e^{-\alpha x/2} + \frac{s_0 e^{-\alpha x}}{j\omega} \quad (B.22)$$

where:

$$\begin{aligned} \alpha &= 300 \text{ m}^{-1} \\ m_0 &= 0.5 \text{ kg.m}^{-2} \\ s_0 &= 1.0 \times 10^9 \text{ kg.m}^{-2} \text{ s}^{-2} \\ r_0 &= \delta_0 m_0 \sqrt{\frac{s_0}{m_0}} \text{ kg.m}^{-2} \text{ s}^{-1} \end{aligned}$$

where δ_0 is approximately equal to the reciprocal of the Q-factor of the resonance peak, here δ_0 is taken equal to 0.4.

- The characteristic frequency, given by the formula:

$$f_c(x) = \frac{1}{2\pi} \sqrt{\frac{s(x)}{m_0}} \quad (B.23)$$

The characteristic frequency of a given point is the frequency at which the velocity amplitude response is a maximum for a given stimulus. This is linked to the characteristic place, where for a given stimulus frequency, the characteristic frequency equals the stimulus frequency. The de Boer model assumes a perfect exponential spatial variation of characteristic frequency (see Fig.13):

$$fc(x) = \frac{1}{2\pi} \sqrt{\frac{s_0}{m_0}} \exp\left(-\frac{\alpha x}{2}\right) \quad (\text{B.24})$$

According to equation (B.23) and the value of the parameters, the lower frequency limit of the model at the helicotrema ($x=L$) is 118 Hz, and so the model is not valid for excitation frequencies below this.

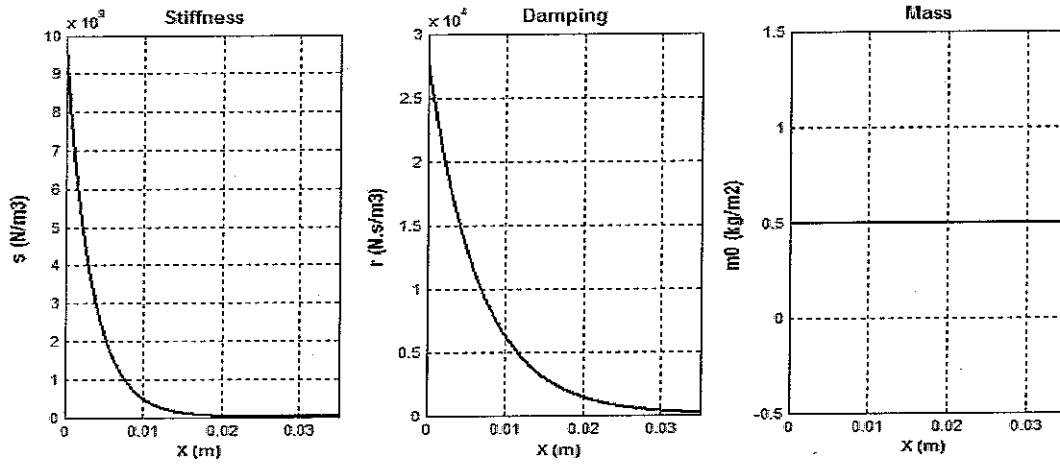


Figure 11: Variations of stiffness, damping and mass along CP (de Boer model)

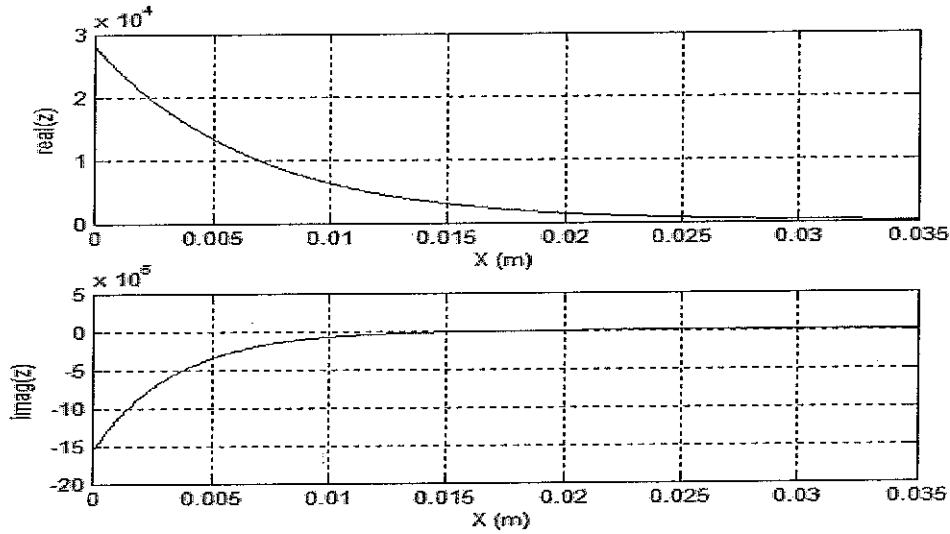


Figure 12: Variations of real and imaginary part of Z_{cp} along CP, at an excitation frequency of 1 kHz (de Boer model)

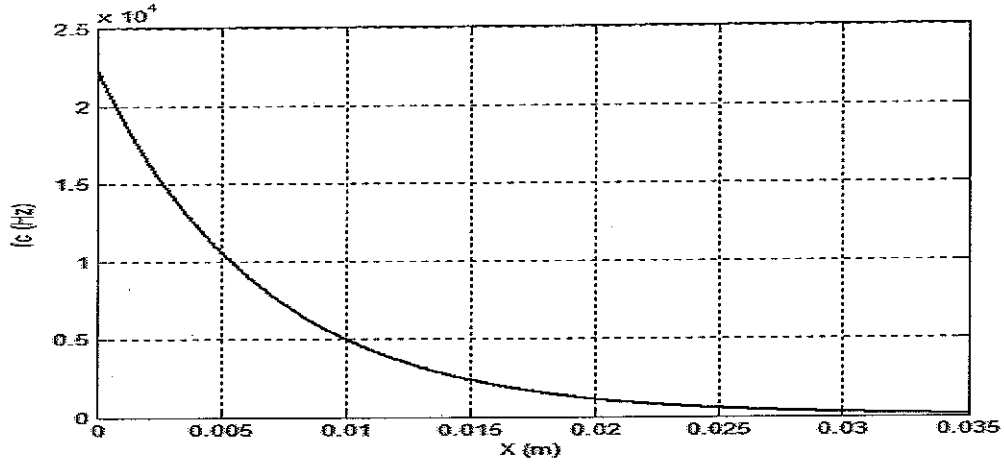


Figure 13: Variations of the characteristic frequency along the CP (de Boer model)

- The wave number of the travelling wave, given by the formula:

$$k_{TW}(x, \omega) = \sqrt{\frac{-2j\omega p}{HZ_{cp}(x, \omega)}} \quad (B.25)$$

and this is plotted in Fig.14 as a function of position along the cochlea for an excitation frequency of 1 kHz

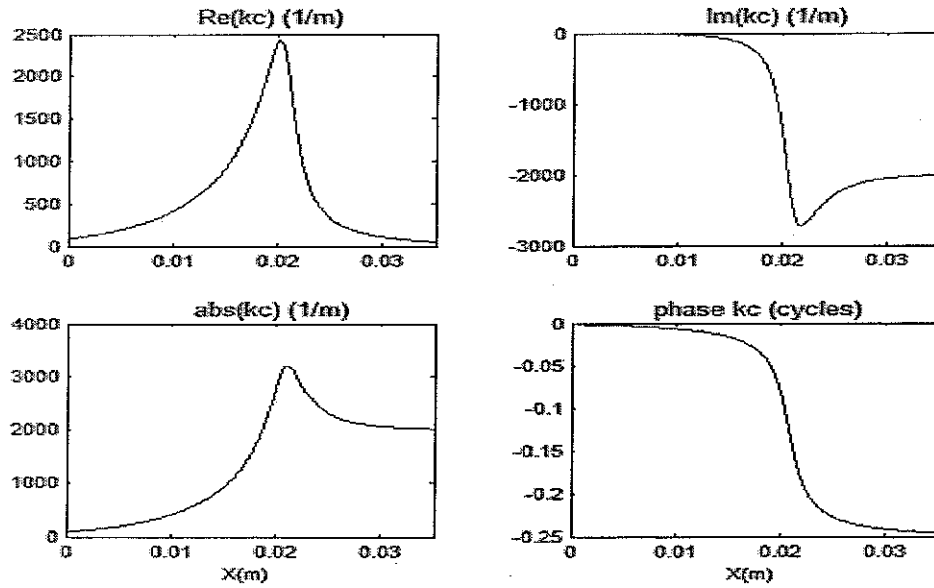


Figure 14: Evolution of k_{TW} with x at 1 kHz (de Boer passive model)

- The wavelength of the travelling wave, given by the formula:

$$\lambda_{TW}(x, \omega) = \frac{2\pi}{k_{TW}(x, \omega)} \quad (B.26)$$

This result is useful because it enables us to locate the portions of cochlea where the long wave approximations break down (i.e. when the criterion $H/\lambda_{TW} \ll 1$ is not respected).

The phase speed of travelling wave (c_{TW}), is given by:

$$c_{TW}(x, \omega) = \frac{\omega}{k_{TW}(x, \omega)} \quad (\text{B.27})$$

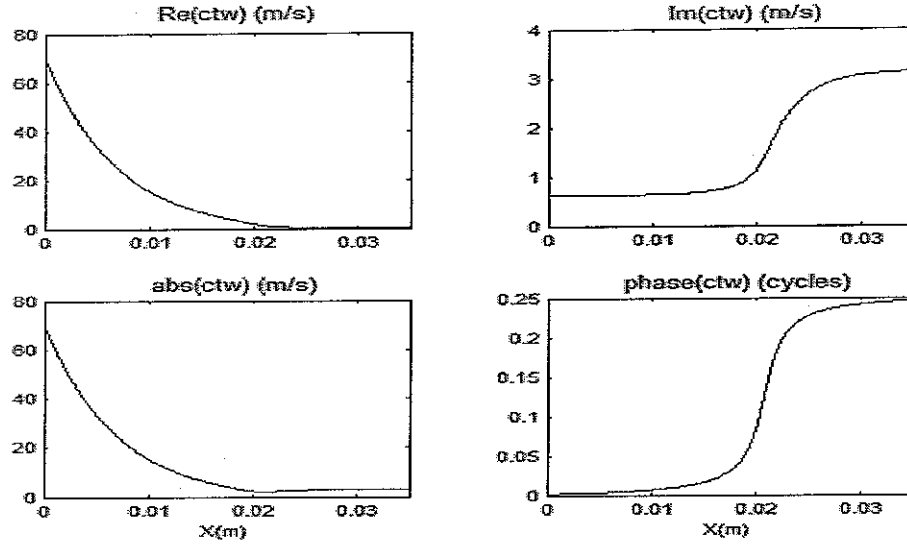


Figure 15: Evolution of the phase speed c_{tw} along the cochlea at an excitation frequency of 1 kHz (de Boer model)

These figures bring some comments:

1. Resistance term is taken to be positive in this model and thus the BM is considered as passive, it can only absorb energy. In active models, BM can be considered as an energy source, resistance will then be negative over a certain domain of x .
2. This impedance model leads to a single frequency wave encountering three regions along x axis, as shown in Fig.14:

a-Near the oval window stiffness dominates, for positions where $0 < x < 0.02$ at an excitation frequency of 1 kHz; the impedance of the cochlear partition is mainly stiffness-controlled, so that:

$$Z_{cp}(x, \omega) \approx \frac{s(x)}{j\omega} \quad 0 < x < 0.02 \quad (\text{B.28})$$

And hence, the wave equation (B.15), can be written:

$$\frac{\partial^2 p_d(x, \omega)}{\partial x^2} + \frac{2\omega^2 \rho}{H \cdot s(x)} p_d(x, \omega) = 0 \quad (\text{B.29})$$

So that the wave number is real and given by:

$$k_{TW}(x, \omega) \approx \omega \sqrt{\frac{2\rho}{H \cdot s(x)}} \quad (\text{B.30})$$

And the solution to the wave equation is a propagating wave, whose phase speed decreases (Fig.15) as it moves along the cochlea, because of the variation of $s(x)$ with x .

b-Where $Z_{cp}(x)$ is nearly real ($x=0.021$ m at 1 kHz), we approach the resonance point, CP velocity is there characterized by a peak and pressure begins decaying. At this point, energy builds up and most of the power of the cochlear wave is dissipated in the BM, which is here totally passive. Moreover the wavelength of the travelling wave reaches its minimum value, in terms of module, thus it is the region where the long-wave approximation is most likely to fail. The module of the phase speed tends also to reach its minimum.

c-After the peak region ($x>0.02$ at 1 kHz), the wave is attenuated very rapidly; the impedance of the CP is dominated by its mass component and thus no longer acts as a potential energy store (mass-controlled region), so that:

$$Z_{cp}(x, \omega) \approx j\omega m(x) \quad x > 0.02 \quad (B.31)$$

And hence, the wave equation is

$$\frac{\partial^2 p_d(x, \omega)}{\partial x^2} - \frac{2\rho}{H.m(x)} p_d(x, \omega) = 0 \quad (B.32)$$

so:

$$k_{TW}(x, \omega) \approx j \sqrt{\frac{2\rho}{H.m(x)}} \quad (B.33)$$

And the solution to the wave equation is an evanescent wave, decaying exponentially. Note that the phase speed is also dominated by its imaginary component.

3. In this model, organ of Corti's influence is neglected, it is assumed to follow the motion of BM. Thus, we use the macromechanical framework of cochlea.

B.2.e. Impedance of the CP, locally active linear long wave models

To some extent, passive models, like the one described above, can be satisfactory to describe cochlear phenomena, as long as the experiments are carried out on dead cochleas. However, such models are unable to provide results that stick to experimental results obtained with live cochlea, for example they can not reproduce the sharpness of the BM displacement near the peak region. The cochlear amplifier proposed by Neely and Kim [3] is an attempt at simulating the high sensitivity and sharp tuning characteristic of the mammalian cochlea. The active elements are postulated to be mechanical force generators that are powered by electrochemical energy of the endolymph, controlled noticeably by the bending of outer hair cells stereocilia. The interest of this model is that active elements are included through the formulation of the impedance of the cochlear partition. The justifications for the formulation of this impedance are detailed later (see *section E*) for more precisions, see [3] as

well. Nevertheless, it is important to mention that the impedance proposed involves an active gain parameter (γ) that can be tuned (usually between 0 and 1) in order to see the influence of the cochlear amplifier, the default value used in [3] is $\gamma=1$.

This version for cochlear partition impedance is:

$$Z_{cp} = \left(\frac{g}{b} \right) \left[Z_1 + Z_2 \frac{(Z_3 - \gamma Z_4)}{(Z_2 + Z_3)} \right] \quad (\text{B.34})$$

The model parameters values are fully detailed in section E where the stability of the lumped component model is studied. Note that the parameters taken by Neely and Kim for their model are those of the cat cochlea, nevertheless that does not affect physical comparison with the passive model of de Boer (human parameters). Yet, we have to mention that the length of the cochlea (L) is taken equal to 35 mm (human cochlea), even though Neely and Kim take $L=25$ mm (cat cochlea). Given that we just want to illustrate the physical properties of the cochlear mechanism, this modification is convenient to compare the several models, furthermore it has no deep consequences on the numerical results.

Kanis and de Boer [2] propose another version of locally active linear impedance, called cochlear amplifier Z_{ca} .

$$Z_{ca} = e_0 d_0 \omega_c(x) \frac{1 + j\beta(x, \omega)}{\delta_{sc} + j[\beta(x, \omega) - \sigma^2 / \beta(x, \omega)]} \quad (\text{B.35})$$

where:

$$\omega_c = \sqrt{\frac{s(x)}{m_0}} \quad \text{and} \quad \beta(x, \omega) = \frac{\omega}{\omega_c} \quad (\text{B.36})$$

with:

- e_0 : active OHC impedance parameter ($\text{kg.m}^{-2}\text{s}$)
- d_0 : active OHC impedance parameter (kg.s^{-1})
- δ_{sc} : Stereocilia damping
- σ : OHC resonance shift ratio

The impedance of CP partition is then, if we call the passive impedance proposed by de Boer (see (B.22)) Z_{pass}

$$Z_{cp} = Z_{pass} - C_{af} * Z_{ca} \quad (\text{B.37})$$

C_{af} being the cochlear amplification factor (if $C_{af}=0$ we have a passive model)

This version of impedance is partly inspired by the one of Neely and Kim [3], adapted to human cochlea. These active models can be characterized by the real parts of Z_{cp} along cochlea; indeed, its sign enables to locate active portions of cochlea, owing to the fact that cochlear amplification occurs when damping is negative. As shown by Fig.16, the locally active models are characterized by an area on the cochlear partition where the real part (damping) is negative, along this part the cochlear partition provides energy to the system.

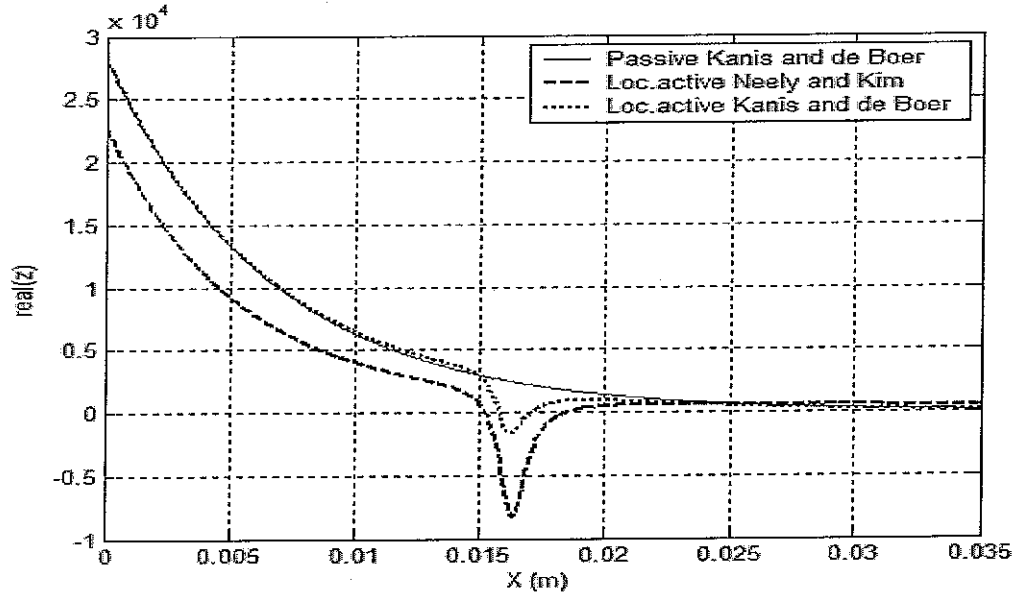


Figure 16: Real part of Z_{cp} for the three different models, at 1000 Hz, $\gamma=1$ and $Caf=1$

B.3. Implementation of the cochlear model using finite difference method

For the sake of the physical clarity, the basilar membrane is pictured as a bank of spring mounted micro-pistons immersed in an inviscid fluid. In view of previous hypothesis, it is possible to start the implementation of a simple passive and one-dimensional model. BM's length (L) is divided into $N-1$ elements, length of which is Δ ($\Delta=L/(N-1)$), thus we use N points to represent cochlea in x dimension, the first point stands for the oval window, the last point stands for the helicotrema. Replacing $\frac{d^2 p_d}{dx^2}$ by its finite difference approximation (using a Taylor development), equation (B.16) can be written as, for i from 2 to $N-1$:

$$\frac{p_d(i+1) - 2p_d(i) + p_d(i-1))}{\Delta^2} - \frac{2j\omega\rho}{H * Z_{cp}(i)} p_d(i) = 0 \quad (\text{B.38})$$

The boundary condition at the base (B.19) can be written using another finite difference approximation:

$$\frac{p_d(2) - p_d(1))}{\Delta} = -2j\omega\rho u_{st} \quad (\text{Base}) \quad (\text{B.39})$$

At the apex, we apply the condition (B.20)

$$p_d(N) = 0 \quad (\text{Apex}) \quad (\text{B.40})$$

The basal boundary condition makes appear the source term in the second member of the equation.

Then, we obtain the following system, taking $\frac{1}{Z_{cp}} = Y_{cp}$

$$\left[\frac{1}{\Delta^2} \begin{pmatrix} -\Delta & \Delta & & & \\ 1 & -2 & 1 & & 0 \\ & \ddots & \ddots & \ddots & \\ & & \ddots & \ddots & \\ 0 & & & 1 & -2 & 1 \\ & & & & 0 & \Delta^2 \end{pmatrix} \right] \frac{2j\omega\rho}{H} \begin{pmatrix} 0 & & & & \\ & Y_{cp}(2) & & & 0 \\ & & \ddots & & \\ & & & Y_{cp}(n-1) & \\ 0 & & & & 0 \end{pmatrix} \begin{pmatrix} p_d(1) \\ \vdots \\ p_d(i) \\ \vdots \\ p_d(N) \end{pmatrix} = \begin{pmatrix} -2j\omega\rho\alpha_{st} \\ 0 \\ \vdots \\ 0 \end{pmatrix} \quad (\text{B.41})$$

This system can be written as:

$$\mathbf{C}\mathbf{P}_d - \mathbf{M}\mathbf{P}_d = \mathbf{S} \quad (\text{B.42})$$

Where \mathbf{C} is the matrix due to fluid coupling, \mathbf{M} is the diagonal mobility matrix, \mathbf{P}_d the pressure array and \mathbf{S} the source array.

Or, equivalently

$$\mathbf{T}\mathbf{P}_d = \mathbf{S} \quad (\text{B.43})$$

\mathbf{T} : tridiagonal matrix ($N \times N$), ($\mathbf{T} = \mathbf{C} - \mathbf{M}$)

Resolve:

$$\mathbf{P}_d = \mathbf{T}^{-1}\mathbf{S} \quad (\text{B.44})$$

In this model, the inversion operation is achieved using MATLAB function *inv()*.

B.4. Results of the cochlear models

B.4.a. Layout of the results

Semi difference pressure

Once obtained the pressure array, the diagram pressure vs position (along cochlear partition) can be plotted, according to the formula:

$$P_{dB} = 10 \log_{10} \left(\frac{P_d}{P_{ref}} \right) \quad (\text{B.45})$$

Where p_{ref} is the reference ($p_{ref} = 2e-5 \text{ Pa}$)

CP velocity

According to equation (B.14), we can infer cochlear partition velocity (v) from the pressure array.

$$v(x, \omega) = \frac{-2p_d(x, \omega)}{Z_{cp}(x, \omega)} \quad (\text{B.46})$$

$$WdB = 10 \log_{10} \left(\frac{v}{v_{ref}} \right) \quad (\text{B.47})$$

where v_{ref} the velocity reference (1 m.s^{-1}).

Note that for each case, WdB and PdB , the references taken are independent of radian frequency (ω).

Fluid velocity

Moreover, the velocity of the fluid can be deduced from the pressure array, using the conservation of the x -momentum (equation (B.5)), in our model, this can be written :

$$u_f(i) = -\frac{p_d(i+1) - p_d(i)}{j\omega\rho\Delta} \quad \text{for } 2 \leq i \leq N-1 \quad (\text{B.48})$$

and for $i=1$, according to(10)

$$u_f(1) = u_f(2) - \frac{v(2)*\Delta}{H} \quad (\text{B.49})$$

In the figures below (from Fig.17 to Fig.23), are presented few results for the three different models. In each figure is presented the response of the model in terms of amplitude of either pressure as defined in equation (B.45), or velocity of the cochlear partition v as defined in equation (B.47); in each case the phase of the parameter is plotted. Each time, 6 curves are plotted, they correspond to the frequencies: 200, 2200, 4200, 6200, 8200 and 10200 Hz respectively from right to left. The velocity at the stapes is kept constant. 1024 points are used to represent the cochlear partition. These data are plotted versus the position (x) along cochlear partition. In each case the amplitude of the stimulus u_{st} is taken equal to 1 ms^{-1} .

B.4.b. Kanis and de Boer passive long wave model

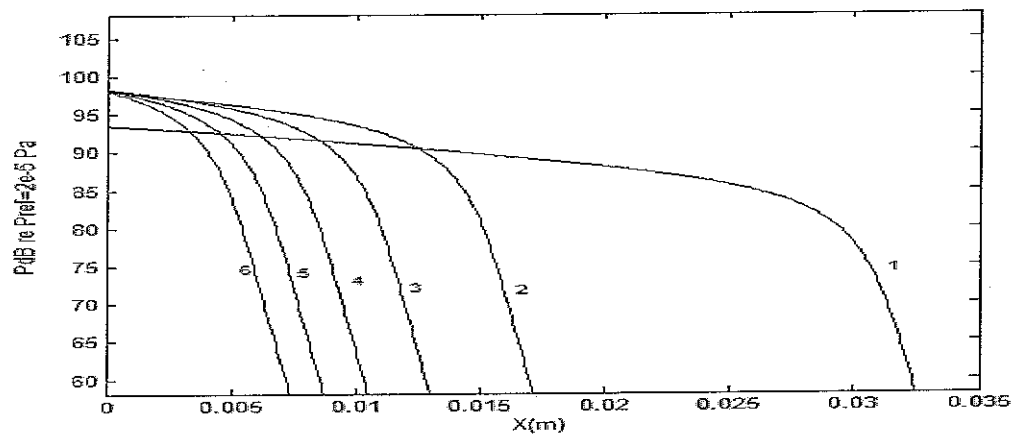


Fig 17.a

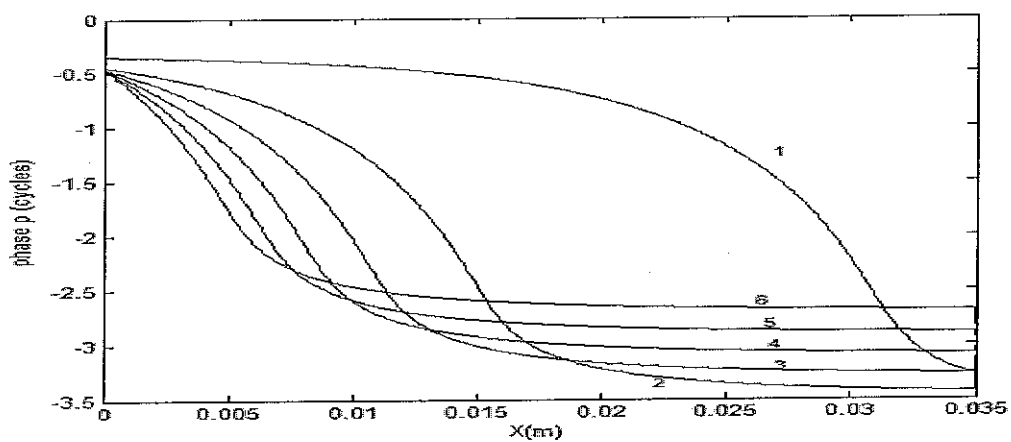


Fig 17.b

Figure 17 (a and b): Pressure (amplitude and phase) for the passive long wave model of de Boer. (1, 2, 3, 4, 5, 6 correspond to 200 Hz, 2200 Hz, 4200 Hz, 6200 Hz, 8200 Hz, 10200 Hz respectively) ,

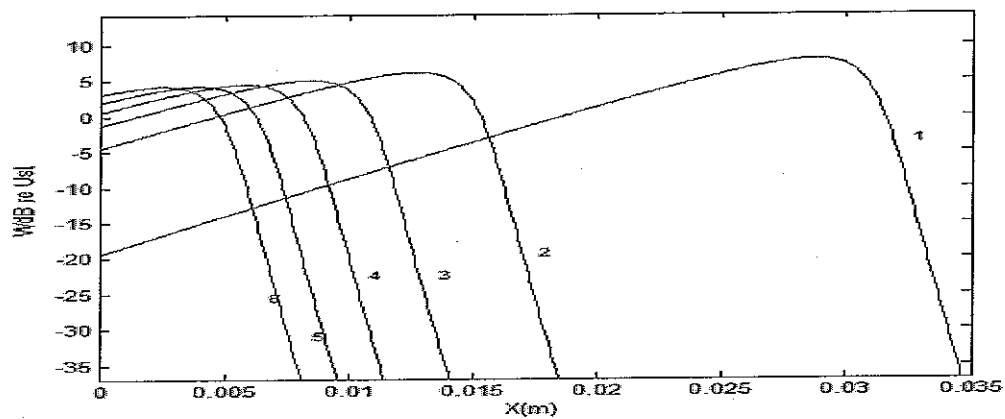


Fig 18.a

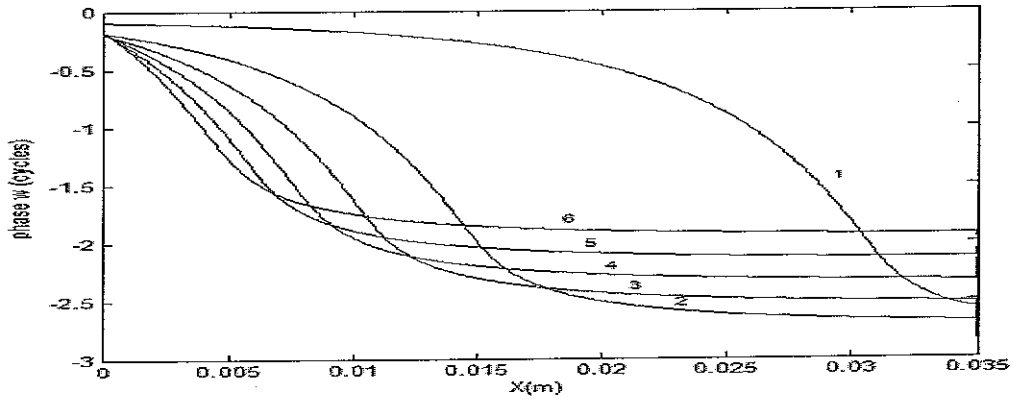


Fig 18.b

Figure 18 (a and b): Velocity of cochlear partition (amplitude and phase) for the passive long wave model of de Boer. (1, 2, 3, 4, 5, 6 correspond to 200 Hz, 2200 Hz, 4200 Hz, 6200 Hz, 8200 Hz, 10200 Hz respectively)

B.4.c. Neely and Kim locally active model

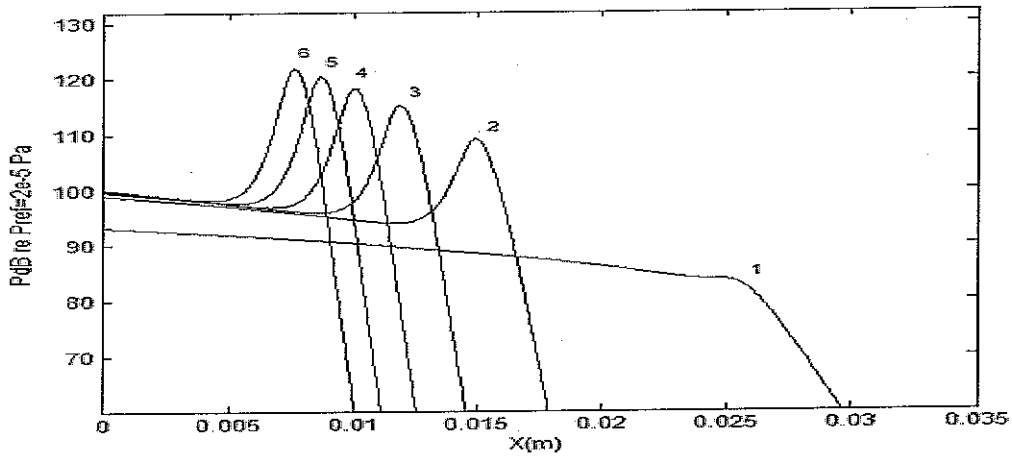


Fig 19.a

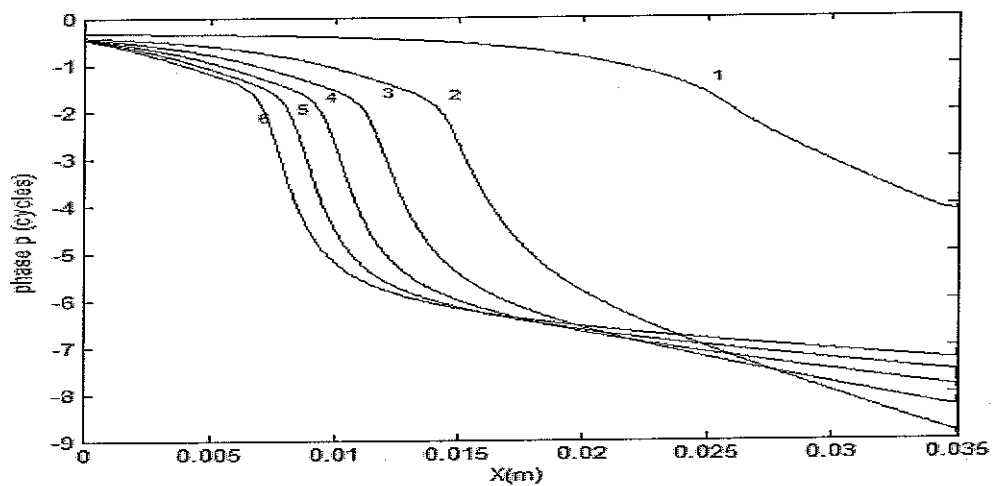


Fig 19.b

Figure 19 (a and b): Pressure (amplitude and phase) for the locally active long wave model of Neely and Kim (active gain $\gamma=1$). (1, 2, 3, 4, 5, 6 correspond to 200 Hz, 2200 Hz, 4200 Hz, 6200 Hz, 8200 Hz, 10200 Hz respectively).

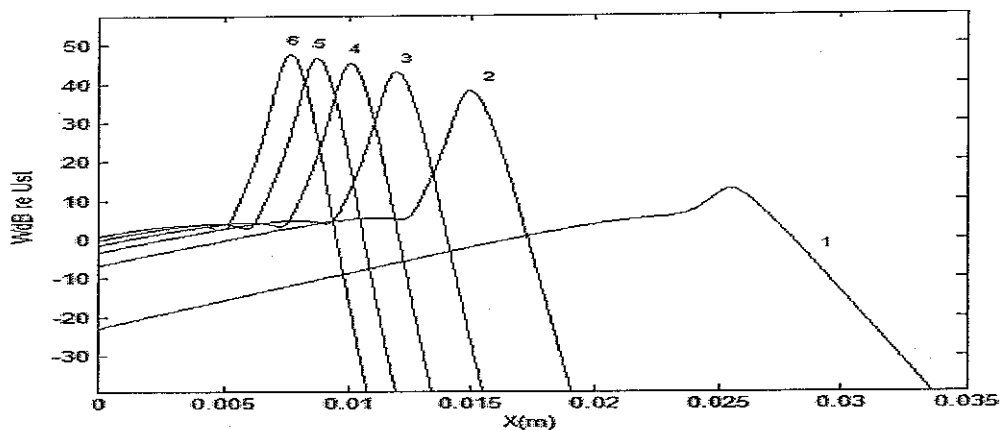


Fig 20.a

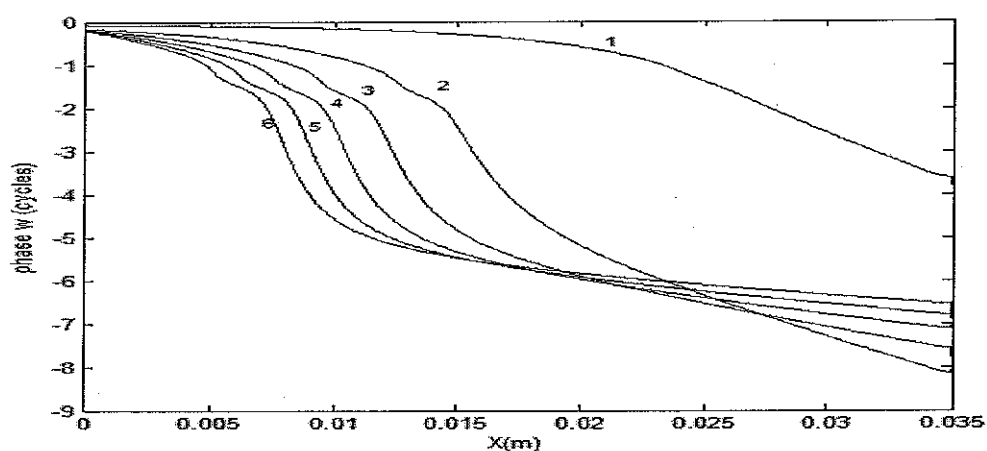


Fig 20.b

Figure 20 (a and b): Velocity of the cochlear partition (amplitude and phase) for the locally active long wave model of Neely and Kim (active gain $\gamma=1$), (1, 2, 3, 4, 5, 6 correspond to 200 Hz, 2200 Hz, 4200 Hz, 6200 Hz, 8200 Hz, 10200 Hz respectively)

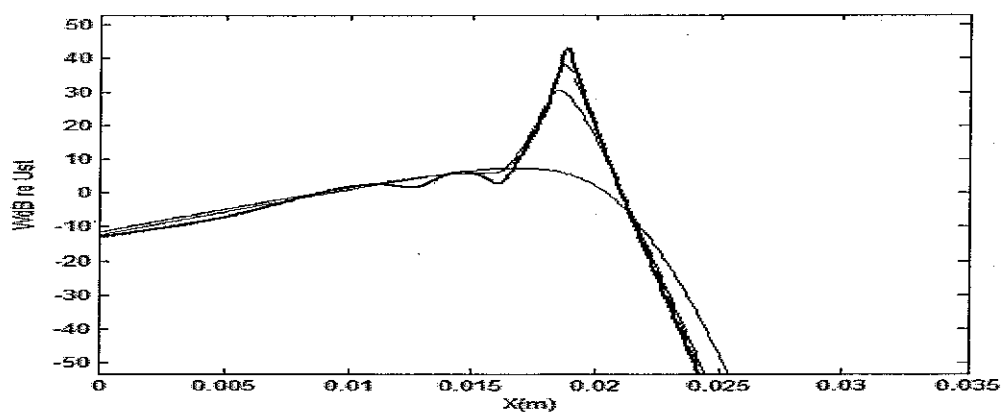


Figure 21: Velocity of the cochlear partition (amplitude and phase) for the locally active long wave model of Neely and Kim, the effect of varying the cochlear amplifier gain γ at 1000 Hz, ($\gamma=0$; 1; 1.1 and 1.15), at this frequency “instabilities” appear for $\gamma=1.15$.

B.4.d. Kanis and de Boer locally active model

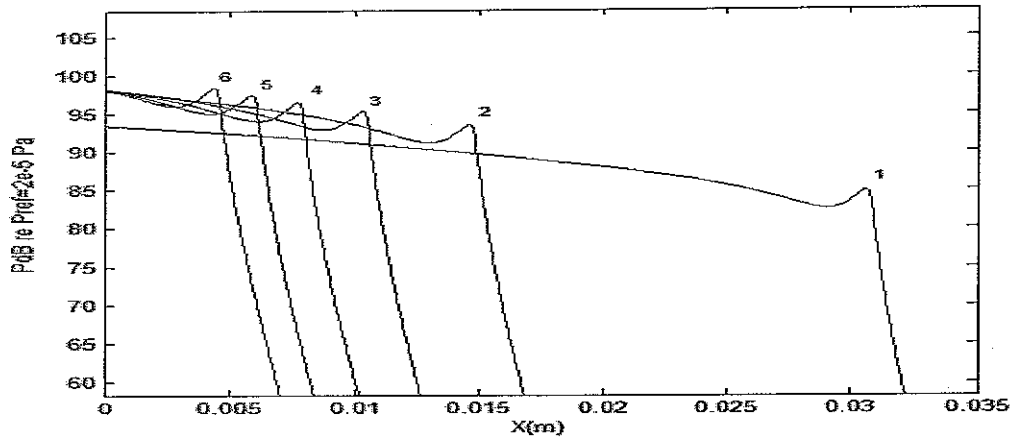


Fig 22.a

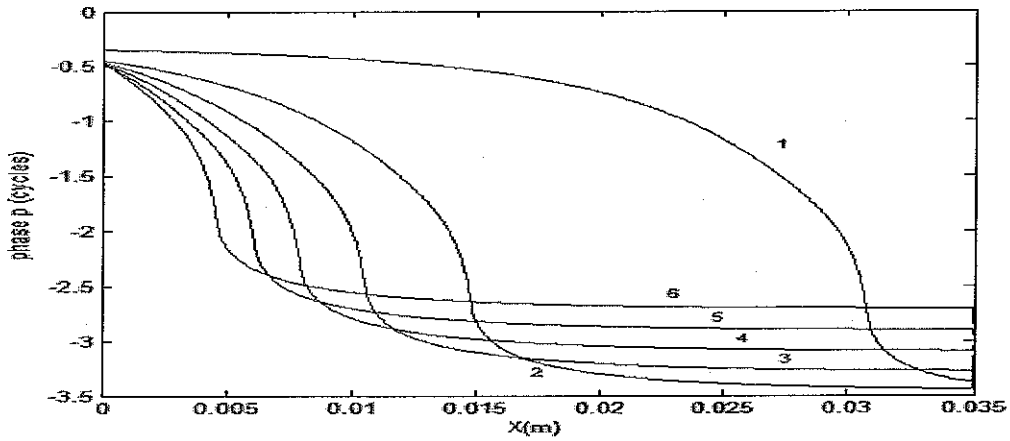


Fig 22.b

Figure 22 (a and b): Pressure (amplitude and phase) for the locally active long wave model of Kanis et al. (cochlear amplification factor $Caf=1$), (1, 2, 3, 4, 5, 6 correspond to 200 Hz, 2200 Hz, 4200 Hz, 6200 Hz, 8200 Hz, 10200 Hz respectively).

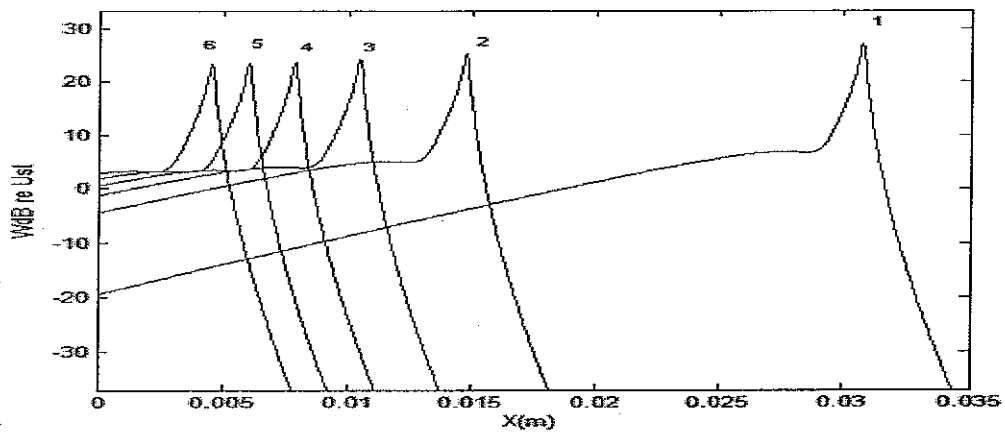


Fig 23.a

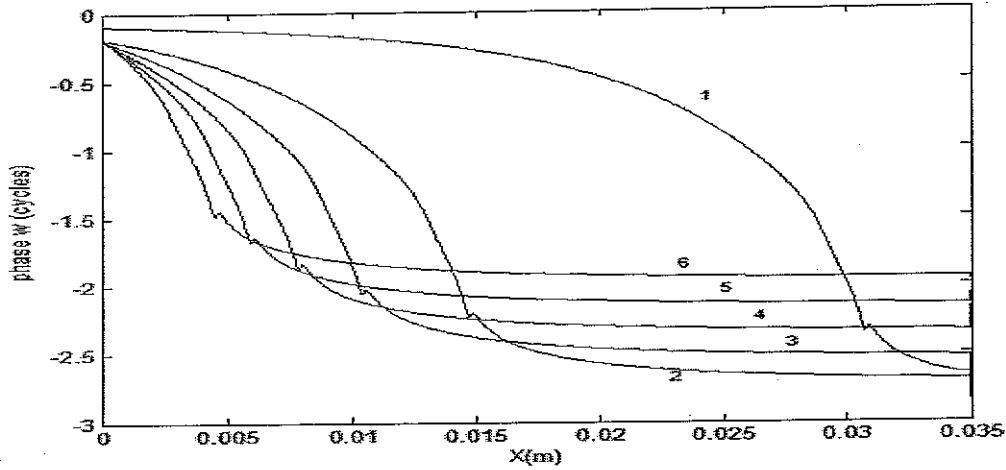


Fig 23.b

Figure 23 (a and b): Velocity of the cochlear partition (amplitude and phase) for the locally active long wave model of Kanis et al. (cochlear amplification factor $Caf=1$), (1, 2, 3, 4, 5, 6 correspond to 200 Hz, 2200 Hz, 4200 Hz, 6200 Hz, 8200 Hz, 10200 Hz respectively).

B.5. Network model of the cochlea

Considering the equations leading the mechanics of the cochlea, one can formulate the model as an electrical network, which is sometimes called the transmission line model. The analogy between the cochlear model and an electrical network is as follows (Fig.24) :

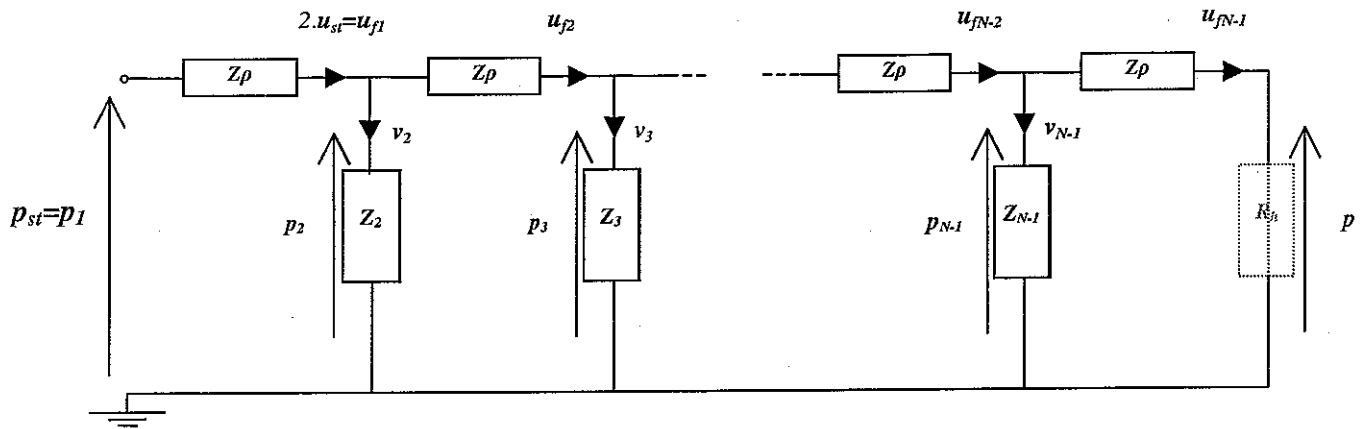


Figure 24: Network model of the cochlea

This network can be used in two ways:

If we are to consider the velocity of the fluid and of the basilar membrane, quantities of the network are as follows:

p_i stands for the semi difference pressure $p_d(i)$

u_{fi} stands for the velocity of the fluid $u_f(i)$

v_i stands for the BM velocity $v(i)$ multiplied by a constant such that:

$$v_i = -\frac{\Delta}{H} v(i) \quad (B.50)$$

Z_p stands for the acoustic impedance of the fluid (constant in all the cross sections) such that:

$$Z_p = j\omega\rho\Delta \quad (\text{B.51})$$

Z_i stands for the cochlear partition impedance $Z_{cp}(i)$ corrected by a constant:

$$Z_i = \frac{H}{2\Delta} Z_{cp}(i) \quad (\text{B.52})$$

R_h stands for the fluid damping that can be considered at the helicotrema, in our case $R_h=0$

p_{st} and u_{st} are the pressure and the velocity of the stapes footplate

Else, if we are to consider the volume velocity of the fluid, and the volume velocity generated by the motion of the basilar membrane, quantities of the network are as follows:

p_i stands for the semi difference pressure $p_d(i)$

u_{fi} stands for the volume velocity of the fluid $u_f(i)$

v_i stands for the volume velocity generated by the BM velocity $v(i)$ multiplied by a constant such that:

$$v_i = -v(i) * W * \Delta \quad (\text{B.53})$$

Z_p stands for the acoustic impedance of the fluid (constant in all the cross sections) such that:

$$Z_p = \frac{j\omega\rho\Delta}{WH} \quad (\text{B.54})$$

where W and H are respectively the width and the height of the upper channel.

Z_i stands for the cochlear partition impedance $Z_{cp}(i)$ corrected by a constant:

$$Z_i = \frac{Z_{cp}(i)}{2 * W\Delta} \quad (\text{B.55})$$

R_h stands for the fluid damping that can be considered at the helicotrema, in our case $R_h=0$

p_{st} and u_{st} are the pressure and the volume velocity of the stapes footplate

This network model is useful to visualize the relationships between the several quantities, and noticeably the relationship between the fluid velocity and the velocity of the basilar membrane. Also, it would be easy to add damping parameter in the fluid impedance, or sources at several points on the cochlea.

C.Validity of the models

C.1. The 'long wave model' criterion

The long wave approximation becomes applicable when the wavelength is much longer than the height of the channel (i.e. $H/\lambda_{TW} \ll 1$). In this case, the fluid y-momentum equation may be ignored, as it has been done in this document in the derivation of the long wave equation. This approximation fails as the wavelength of the travelling wave becomes smaller than the height of the cochlear channel, which occurs in the region of the peak of the travelling wave envelope. The following curves (Fig.25 to Fig.27) present the behaviour of this criterion along the CP for the three models at the same frequencies as above.

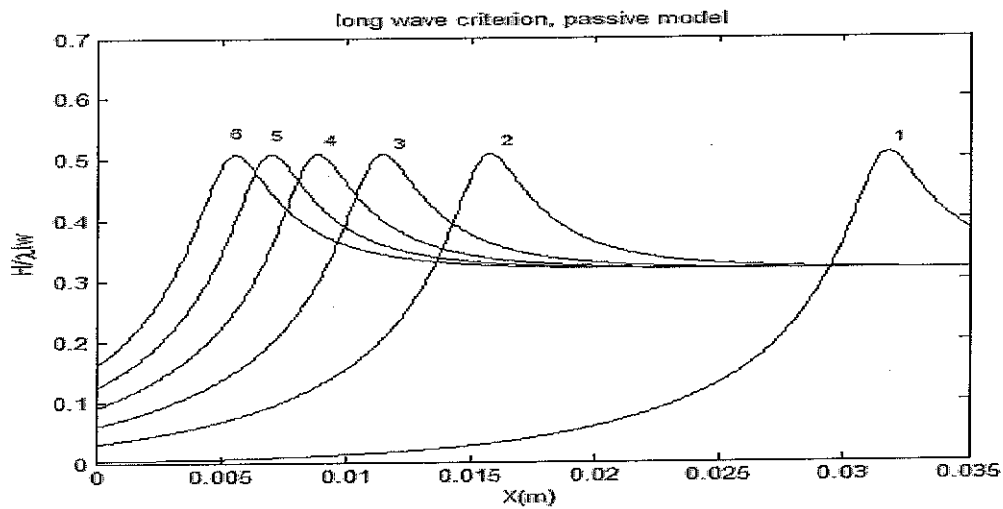


Figure 25: Long wave criterion using de Boer passive model (1, 2, 3, 4, 5, 6 correspond to 200 Hz, 2200 Hz, 4200 Hz, 6200 Hz, 8200 Hz, 10200 Hz respectively)

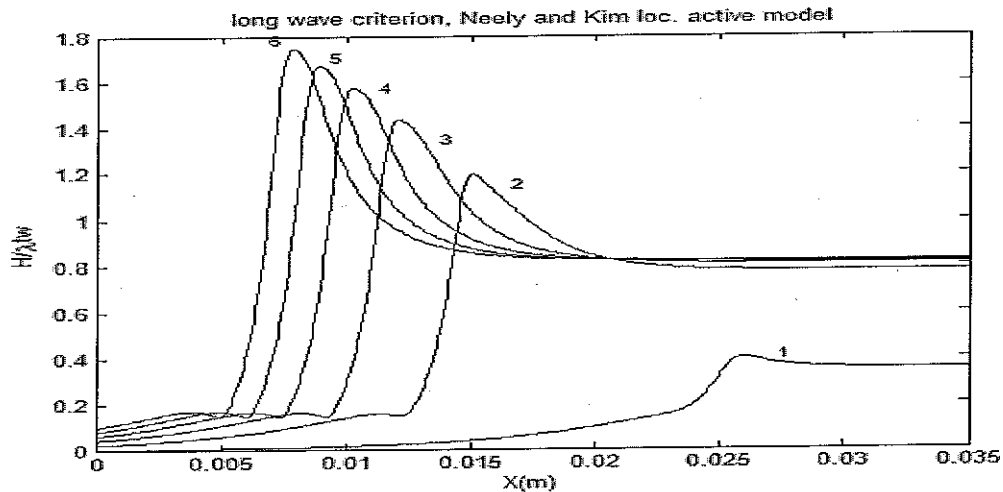


Figure 26: Long wave criterion using Neely et al. locally active model (active gain $\gamma=1$), (1, 2, 3, 4, 5, 6 correspond to 200 Hz, 2200 Hz, 4200 Hz, 6200 Hz, 8200 Hz, 10200 Hz respectively)

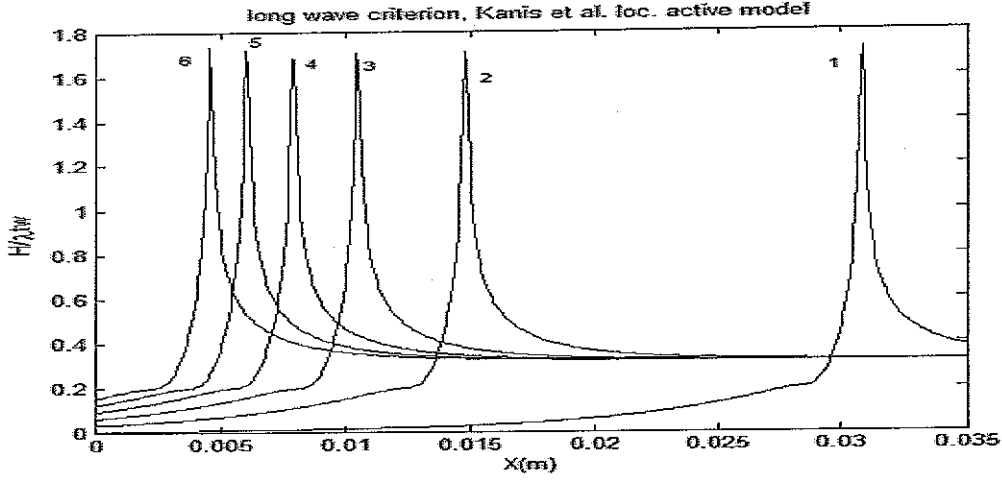


Figure 27: Long wave criterion using Kanis et al. locally active model (cochlear amplification factor $Caf=1$), (1, 2, 3, 4, 5, 6 correspond to 200 Hz, 2200 Hz, 4200 Hz, 6200 Hz, 8200 Hz, 10200 Hz respectively).

Those results allow us to say that the long wave criterion is, on the whole, well respected along cochlear partition. Problems occur, as expected, near the peak region in particular for the two locally active models. To some extent, this does not seem to be a fatal shortcoming, indeed this type of model are used for predicting several kind of oto-acoustic emissions, and these are well predicted as long the longwave model qualitatively captures all the features of the travelling wave that are essential for OAE generation, this according to [7].

C.2. Convergence of the model

C.2.a. Analytic evaluation

Models proposed below are described using a finite difference equation, thus we use a one-dimensional mesh to describe the cochlea. Consequently, it is necessary to determine the minimal number of points that are necessary to describe in the x -direction the cochlea so that the response of the model is reliable. Usually the criterion adopted is to get least 6 points to describe a wavelength of the signal treated:

$$\Delta \leq \frac{\lambda}{6} \quad (C.1)$$

where Δ is the discretization step in the x -direction, and λ is the wavelength of the signal.

In the models presented in this document, the wavelength of the travelling wave (λ_{TW}) follows the relation:

$$\lambda_{TW}(x, \omega) = 2\pi \sqrt{\frac{HZ_{cp}(x, \omega)}{-2j\omega\rho}} \quad (C.2)$$

This expression being rather complicated, because of its dependence with x and ω and the expressions of $Z_{cp}(x, \omega)$, it is rather difficult to determine analytically the expression of the minimal value of λ_{TW} for each of these models, consequently this is determined numerically. The following table (Table 1) gives the minimal values of λ_{TW} (whatever are the position x

and the radian frequency ω). The third column gives the maximal value for Δ according to the criterion (C.1); the fourth column gives the value of N_s (number of points to describe the cochlea in the x -direction), corresponding to the formula

$$N_s = \frac{L}{\Delta} + 1 \quad (\text{C.3})$$

where L is the length of the cochlea (35 mm), this fourth column gives the minimal values for Δ that are “theoretically” required for the convergence of each corresponding model.

Formulation of the impedance	minimum of λ_{TW} (mm)	maximal value for Δ (mm)	minimum for N_s
Kanis and de Boer passive model	1.97	0.38	107
Neely and Kim loc. active model*	0.5	0.083	422
Kanis and de Boer loc. active model**	0.58	0.097	361

* $\gamma=1$, ** $Caf=1$

Table 1

C.2.b.Numerical evaluation

In order to be cautious, these results are checked numerically. The following figures illustrate the evolution of the response in terms of pressure, for several stimulus frequencies; for each of these frequencies, we calculate the evolution with N_s of the pressure response where the travelling wave reaches its minimum in terms of wavelength λ_{TW} (near the peak point of the response). The model is considered as convergent when $PdB(N_s) = PdB(N_{s\infty}) \pm 1$ dB; $N_{s\infty}$ is here equal to 1200.

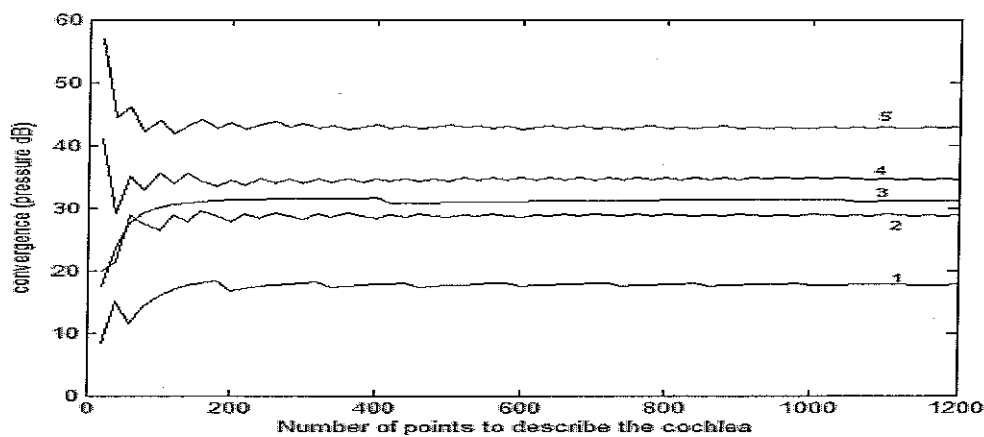


Figure 28: Convergence of the Kanis and de Boer passive model at the peak point, at five frequencies (1, 2, 3, 4 and 5 corresponding respectively to 200 Hz, 5200 Hz, 10200 Hz, 15200 Hz and 20200 Hz), model converges above 200 points.

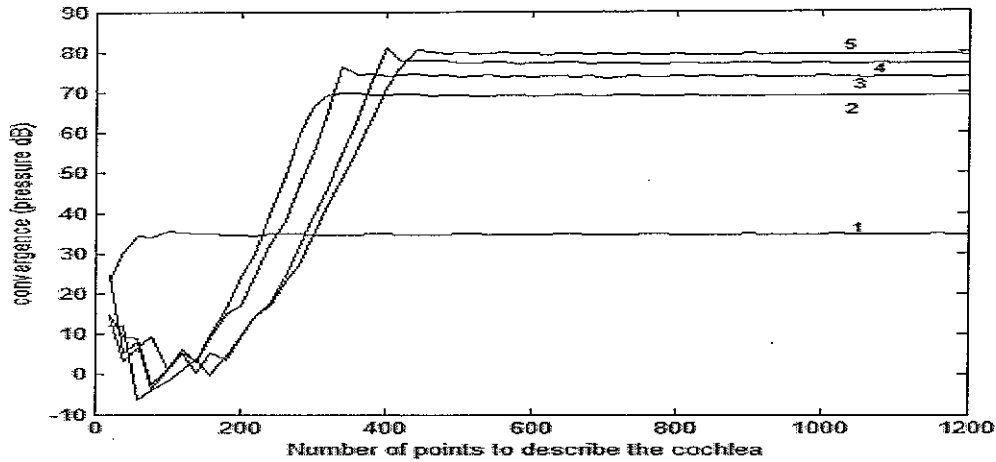


Figure 29: Convergence of the Neely and Kim loc.active model ($\gamma=1$) at the peak point, at five frequencies (1, 2, 3, 4 and 5 corresponding respectively to 200 Hz, 5200 Hz, 10200 Hz, 15200 Hz and 20200 Hz). The model converge above 450 points.

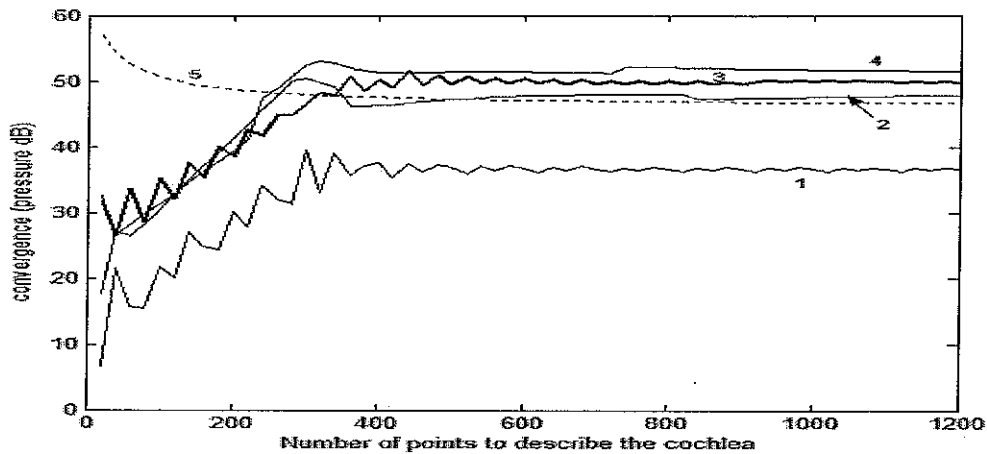


Figure 30: Convergence of the Kanis and de Boer loc.active model ($Caf=1$) at the peak point, at five frequencies (1, 2, 3, 4 and 5 corresponding respectively to 200 Hz, 5200 Hz, 10200 Hz, 15200 Hz and 20200 Hz). The model converge above 400 points.

These several figures are given for only five frequencies, but they are fully representative of the whole behaviour of the convergence of these models. Consequently, we can estimate the minimal values of N_s for each model, considering a variation of ± 1 dB as a satisfactory criterion. The conclusion is: the value $N_s=500$ will be considered as a minimal value for the computation of these models, below 500 points one can not expect reliable results.

C.3. Check of the 'reciprocity' of the model

C.3.a.Principle

The purpose of this section is to examine the 'reciprocity' of the mechanical response of the passive model, and of the locally active models. Namely, the principle of vibrational reciprocity states that the response of a linear elastic system to a disturbance, which is applied at some point by an external agent, is invariant with respect to exchange of the points of input and observed response (Fahy[5]). In our model, reciprocity can be checked in two ways, first it can be analytically assessed taking into consideration the semi-difference pressure p_d and

the volume velocity of the fluid associated with u_f we call it “reciprocity within the fluid”, in a second time, it will be evaluated considering p_d and the volume velocity generated by the motion of a component of the cochlear partition (velocity v), we call it “reciprocity within the cochlear partition”.

C.3.b. Reciprocity within the fluid

The network model of the cochlea (Fig.24) allows to consider that the model is built from a cascade of sections as in Fig.31

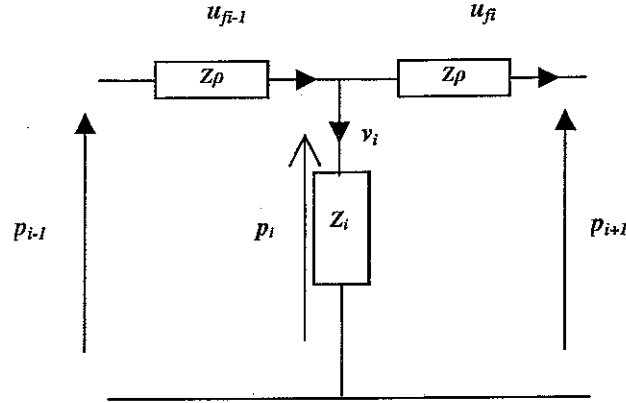


Figure 31: Section of the network model of the cochlea

This can be formulated using the 2-port network analysis, giving the relationship between (p_{i-1}, u_{fi-1}) and (p_{i+1}, u_{fi})

$$\begin{bmatrix} p_{i-1} \\ u_{fi-1} \end{bmatrix} = \begin{bmatrix} T_{11} & T_{12} \\ T_{21} & T_{22} \end{bmatrix} \begin{bmatrix} p_{i+1} \\ u_{fi} \end{bmatrix} \quad (C.4)$$

where

$$\begin{aligned} T_{11} &= \frac{Z_\rho + Z_i}{Z_i} & T_{12} &= Z_\rho \left(2 + \frac{Z_\rho}{Z_i} \right) \\ T_{21} &= \frac{1}{Z_i} & T_{22} &= 1 + \frac{Z_\rho}{Z_i} \end{aligned} \quad (C.5)$$

A way to check the reciprocity of a two port-network model is to proceed as follows. First, we assume that $u_{fi}=0$, and we calculate the report $p_{i+1}/u_{fi-1}|_{u_{fi}=0}$, then we assume $u_{fi-1}=0$, and we calculate $p_{i-1}/u_{fi}|_{u_{fi-1}=0}$, and then we compare both results, that amounts to compare the following quantities:

$$1/T_{21} (P_{i+1}/u_{fi-1}|_{u_{fi}=0}) \text{ and } T_{12} - T_{11} \cdot T_{22} / T_{21} (P_{i-1}/u_{fi}|_{u_{fi-1}=0})$$

If the system is reciprocal, we have

$$P_{i+1}/u_{fi-1}|_{u_{fi}=0} = P_{i-1}/u_{fi}|_{u_{fi-1}=0} \quad (C.6)$$

This boils down to show that

$$T_{11}T_{22} - T_{21}T_{12} = 1 \quad (C.7)$$

Consequently, the 2-port network system is reciprocal if the determinant of the two-port network matrix is equal to 1.

Equation (C.7) is checked by the components T_{11} , T_{12} , T_{21} and T_{22} ; as a result the section presented in Fig.31 is reciprocal. In this case we have considered the velocity of the fluid u_f ; given that, in our model, the cross sectional area of the upper channel is taken constant, the reciprocity is also checked considering not the velocity but the volume velocity of the fluid. However, one should bear in mind that this reciprocal property is conditioned by the fact that the dimensions of the upper channel (in terms of width W and height H) are taken constant in our model.

The demonstration below can be extended to the N section of the cochlear network, that come to multiply N 2-port network matrices as the one described below. Consequently this model is reciprocal considering the quantities characterizing the fluid.

C.3.c. Reciprocity within the cochlear partition

The aim of this section is to exhibit that the system is also reciprocal when we consider the semi-difference pressure and the volume velocity associated with the motion of a lumped component of the model. This reciprocity is possibly equivalent to the previous one, but we did not manage to show it analytically, thus we check it numerically. In our model of the cochlea, we will check the reciprocity taking two points on the membrane A and B , located at the index a and b respectively, applying successively a disturbance (res. S_a and S_b) at this two points. Then we will “measure” using our model the semi difference pressure in the upper channel (p_d) and the velocity of the displacement of cochlear partition (CP) at point A (res. B), when the disturbance is imposed at B (res. A)(see Fig.32).

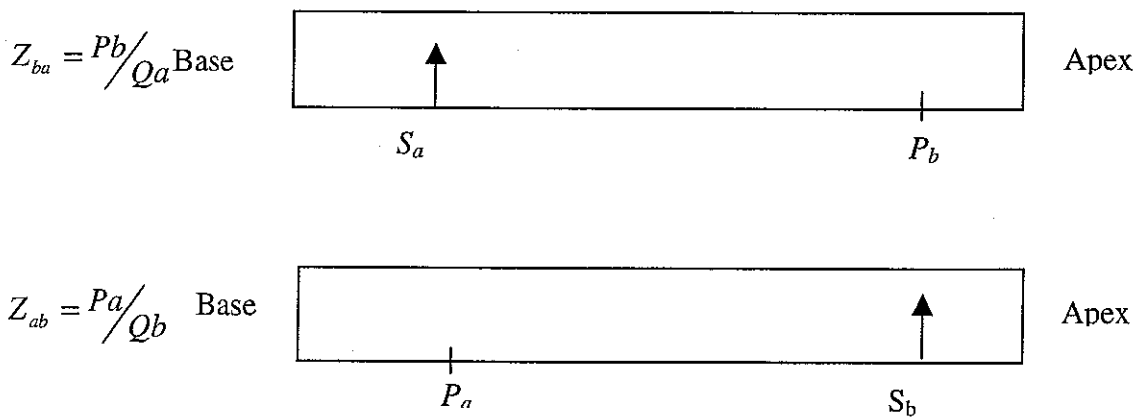


Figure 32: Reciprocity principle

Once we have the response of the model for the two configurations, we can compare the reports Z_{ab} and Z_{ba} .

Equations

In order to calculate those quantities, we have just modified the main equation of the model, that leads to a modification of the source array in the matrix system, so that we obtain:

$$\left[\frac{1}{\Delta^2} \begin{pmatrix} -\Delta & \Delta & & & \\ 1 & -2 & 1 & & 0 \\ & \ddots & \ddots & \ddots & \\ & & \ddots & \ddots & \ddots \\ & & & 1 & -2 & 1 \\ & & & & 0 & \Delta \end{pmatrix} \right] \frac{2i\omega\rho}{H} \begin{pmatrix} 0 \\ Y_{cp}(2) & & 0 \\ & \ddots & & \\ & & Y_{cp}(N-1) & \\ 0 & & & 0 \end{pmatrix} \begin{pmatrix} p_d(1) \\ \vdots \\ p_d(i) \\ \vdots \\ p_d(N) \end{pmatrix} = \begin{pmatrix} 0 \\ \vdots \\ S_i \\ 0 \\ \vdots \\ 0 \end{pmatrix} \quad (C.8)$$

S_i being S_a and S_b successively, with $1 \leq i \leq N$.

Nature of the disturbance

To be in conformity with the model, disturbances are time harmonic quantities.

If $i = 1$, the disturbance is the motion (in x direction) of the stapes footplate, its dimension is ($\text{kg.m}^{-2}.\text{s}^{-2}$). In that case:

$$S_1 = -2i\omega\rho u_{st} \quad (C.9)$$

u_{st} being the velocity of the stapes footplate in the x direction.

In terms of volume velocity, this disturbance S_1 can be written as

$$S_1 = -2i\omega\rho \frac{Q_{st}}{A_{st}} \quad (C.10)$$

where Q_{st} is the volume velocity of the stapes, and A_{st} the area of the stapes.

If $i > 1$, in order to cautiously formulate this source, we go back to the wave equation that govern the pressure field in the fluid at the position x , where the source $S(x, \omega)$ acts

$$\frac{\partial^2 p_d(x, \omega)}{\partial x^2} - \frac{2j\omega\rho}{HZ_{cp}(x, \omega)} p_d(x, \omega) = S(x, \omega) \quad (C.11)$$

Actually, the source term in the wave equation (C.11) can be written as follows

$$S(x, \omega) = -\rho \frac{\partial q(x, \omega)}{\partial t} \quad (C.12)$$

where q is a flow term which dimension is (s^{-1})

In this case, the flow term q is closely linked to $v(x, \omega)$, the velocity of the basilar membrane (m.s^{-1}). First we consider that the fluid motion involved by $v(x, \omega)$ is equivalent to a volume velocity injection in the upper channel. Given the dimensions of a lumped component $W^*\Delta$,

where W and Δ are respectively the width and the length of the lumped component, we can say that the volume velocity $Q(x, \omega)$ corresponding to this lumped component is:

$$Q(x, \omega) = v(x, \omega) * W * \Delta \quad (C.13)$$

Note that this motion acts *a priori* in the z -direction, nevertheless, given that motion of the fluid in the z -direction is neglected, and that the fluid is incompressible, we consider that this fluid motion is spontaneously transmitted in the x direction. Consequently the flow term generated is equivalent to:

$$q(x, \omega) = \frac{Q(x, \omega)}{W * H * \Delta} \quad (C.14)$$

where $W * H * \Delta$ stands for the elementary volume associated to the lumped component (H being the height of the upper channel)
Consequently, for $i > 1$

$$S_i = -i\omega\rho \frac{Q_i}{W.H.\Delta} \quad (C.15)$$

First analysis

In order to check the reciprocity within the cochlear partition, we proceed as follows:

- Point A is kept still, and point B goes all along the cochlear partition
- The level of the disturbance (S_a) at point A is kept constant, its value is chosen by user, at point B q_b follows a random law of Matlab (this is in order to check that reciprocity is independent of the level of S_b).
- For each location of B, Z_{ab} and Z_{ba} and the ratio $R = Z_{ab}/Z_{ba}$ are calculated

Results

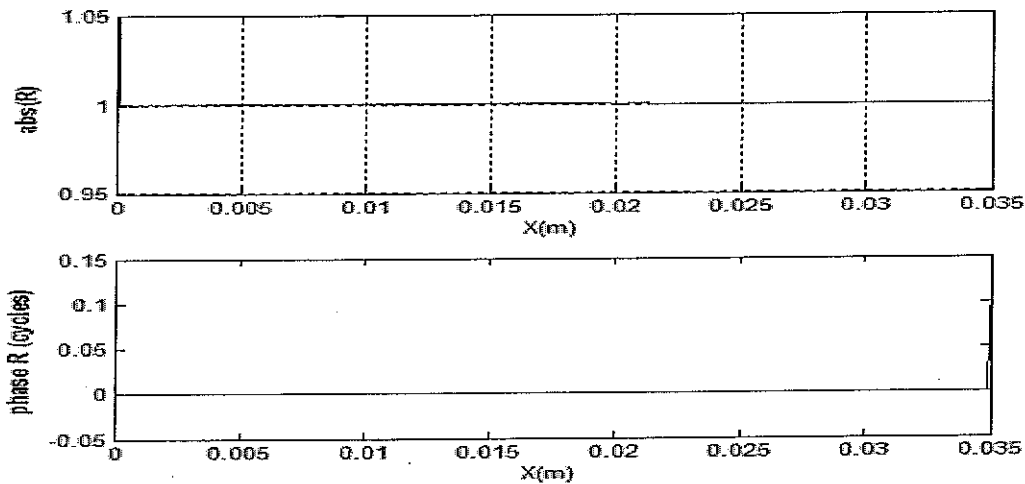


Figure 33: Reciprocity principle checked at 1 kHz, CP is described by 512 points, point A is at $a=20$, point B goes all along the CP ($1 \leq b \leq N$), using de Boer long wave passive model

As we can see in Fig.33, reciprocity is checked for all positions of B, except for $b=1$. This is due to the boundary conditions at the helicotrema. The same results are observed for the two locally active models, taking the same conditions.

Second analysis

For this second analysis, A and B are fixed, the frequency goes from 200 Hz to 20000 Hz, the levels q_a and q_b are constant with frequency.

Results

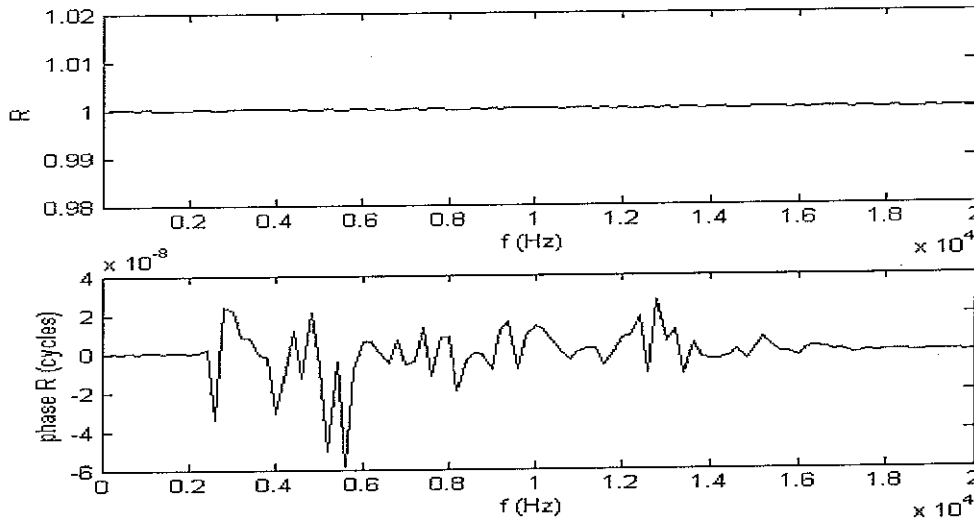


Figure 34: Ratio R at several frequencies (amplitude and phase from 200 to 20000 Hz, with a step of 200 Hz), CP is described by 512 points, point A is at $a=10$, point B at $b=340$, q_a (dB re 1)= 1, q_b (dB re 1)= 5 . Using de Boer passive long wave model.

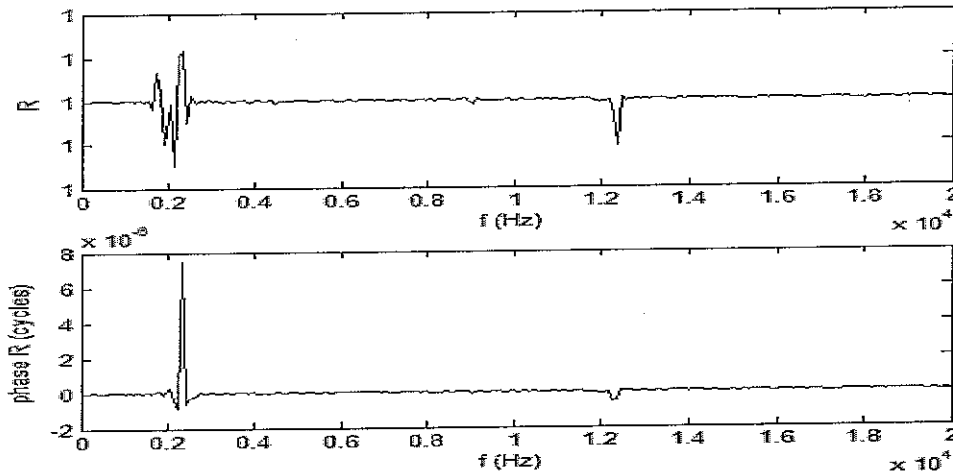


Figure 35: Ratio R at several frequencies (amplitude and phase from 200 to 20000 Hz, with a step of 200 Hz), CP is described by 512 points, point A is at $a=1$, point B at $b=340$, q_a (dB re 1)= 1, q_b (dB re 1)= 5 . Using de Boer passive long wave model.

As we can see in Fig.34, reciprocity is observed at all frequencies using de Boer passive long wave model. The same results are observed for the two locally active models, taking the same conditions. Fig.35 shows that this is noticeably observed when A takes the basal position. Consequently, the reciprocity of the model is observed between the stapes and every point along the cochlea.

D.Build of a comprehensive model of the ear

A model of the middle ear and of the ear canal are required to complete a full mathematical model of the ear, and allow, in particular, OAE in the ear canal to be predicted. The middle ear and ear canal can be represented by a two port network, so that:

$$\begin{bmatrix} p_{ec} \\ Q_{ec} \end{bmatrix} = \begin{bmatrix} T_{ecst11} & T_{ecst12} \\ T_{ecst21} & T_{ecst22} \end{bmatrix} \begin{bmatrix} p_{st} \\ Q_{st} \end{bmatrix} \quad (D.1)$$

where p and Q are the acoustic pressure and the acoustic volume velocity respectively, subscripts ec and st indicate location at the entrance to the ear canal and stapes footplate respectively, the matrix elements T_{ecstij} define the transmission through the ear canal and middle ear.

D.1. Ear canal and middle ear representations

D.1.a. The ear canal model

The ear canal is modeled as a duct, its walls, with the exception of the eardrum, are considered rigid, the viscous thermal damping within this duct is negligible. Sound waves are considered plane, that means that this model will be relevant up to the cut-off frequency of the duct (fc). This model gives us the relations between the quantities at the entrance to the ear canal, and close to the eardrum. The length of this duct is L_{ec} (2cm), and diameter is constant (d). Mathematically it is modelled using a two port network representation. In our model, the cut-off frequency of the ear canal is

$$fc = c_0 / 2d \quad (D.2)$$

where c_0 is the sound speed in the air (340 ms^{-1}) and d the diameter of the ear canal. Given that the cross sectional area of the ear canal (A_{ec}) is around 40 mm^2 (see [8]), d is nearly equal to: 7 mm , the cut off frequency of the model of the ear canal is roughly 24000 Hz, so that the plane wave assumption can be considered as respected in the frequency range 20-20000 Hz.

Consequently, the ear canal model is as follows:

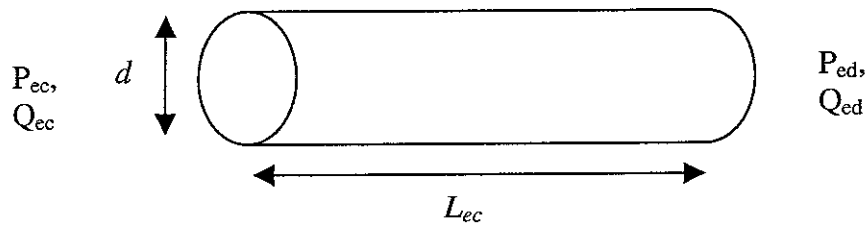


Figure 36: Model of the ear canal

The transfer matrix T_{ec} corresponding to this representations is such that:

$$\begin{bmatrix} P_{ec} \\ Q_{ec} \end{bmatrix} = \begin{bmatrix} T_{eced11} & T_{eced12} \\ T_{eced21} & T_{eced22} \end{bmatrix} \begin{bmatrix} P_{ed} \\ Q_{ed} \end{bmatrix} \quad (D.3)$$

where the components T_{ecedij} are derived from the plane wave theory;

$$\begin{aligned} T_{eced11} &= T_{eced22} = \cos(k.L_{ec}) \\ T_{eced12} &= \frac{j.\sin(k.L_{ec}).\rho_0.c_0}{A_{ec}} \\ T_{eced21} &= \frac{j.\sin(k.L_{ec}).A_{ec}}{\rho_0.c_0} \end{aligned} \quad (D.4)$$

This representation is used by Egolf *et al.* in [9], with the exception that we adopt a constant value cross-sectional area for the ear canal (A_{ec}).

D.1.b. The middle ear model

For the middle ear model, we use the network model for the human middle-ear proposed by Kringlebotn (1988) [6]. This network model is derived to obtain a two port network formulation of the middle ear, so that we obtain the following relations between the pressure and the volume velocity at the eardrum (P_{ed} and Q_{ed}), and at the stapes respectively (P_{st} and Q_{st}).

$$\begin{bmatrix} P_{ed} \\ Q_{ed} \end{bmatrix} = \begin{bmatrix} T_{edst11} & T_{edst12} \\ T_{edst21} & T_{edst22} \end{bmatrix} \begin{bmatrix} P_{st} \\ Q_{st} \end{bmatrix} \quad (D.5)$$

where the values of T_{edstij} in the transfer matrix are strongly frequency dependent. This model is as follows, values of the parameters are given in Table 2:

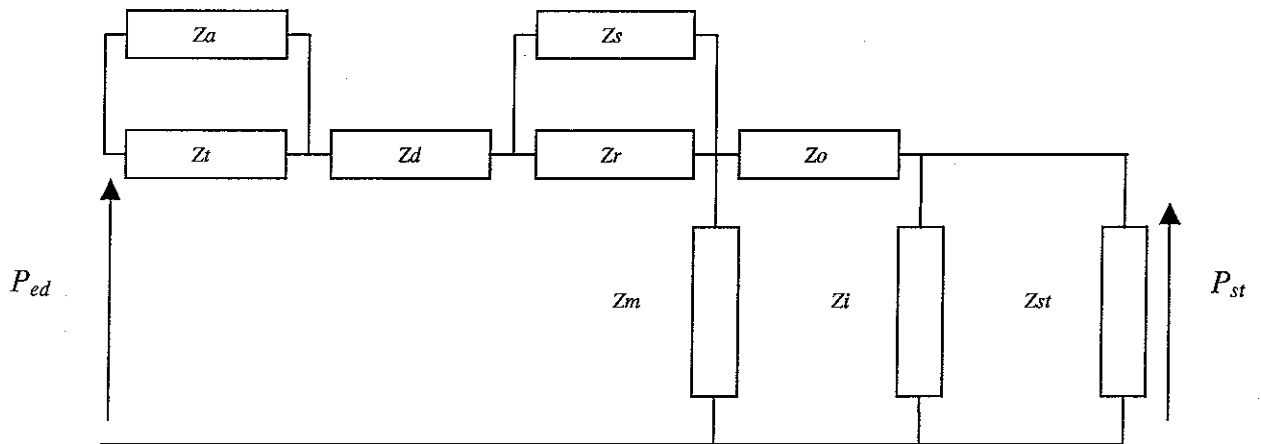


Figure 37: Network model for human middle ear

$$\begin{aligned}
Z_a &= R_a + i\omega L_a + 1/(i\omega C_a) \\
Z_t &= 1/(i\omega C_t) \\
Z_d &= i\omega L_d \\
Z_s &= R_s + i\omega L_s + 1/(i\omega C_s) \\
Z_r &= R_r + i\omega L_r + 1/(i\omega C_r) \\
Z_m &= R_m + i\omega L_m + 1/(i\omega C_m) \\
Z_o &= R_o + i\omega L_o + 1/(i\omega C_o) \\
Z_i &= R_i + 1/(i\omega C_i) \\
Z_{st} &
\end{aligned}$$

a : antrum and mastoid cells
t : tympanic cavity
d : drum
s : suspension of the eardrum
r : rim of eardrum
m : coupling between malleus and incus
o : ossicles (malleus and incus)
i : coupling between incus and stapes
st : input impedance of the cochlea

It can be more simply presented as a block diagram:

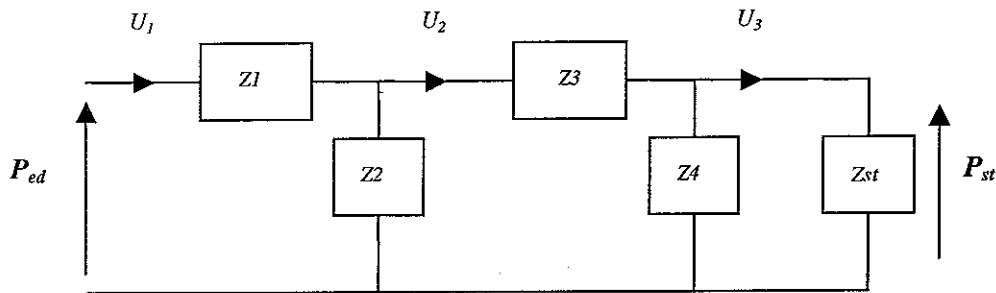


Figure 38: Block diagram for the middle ear

where U_1 and U_3 are Q_{ed} and Q_{st} respectively.

Compared to the model proposed by Kringlebotn, a slight difference has been brought; in our case the influence of the cochlea is fully taken into account through Z_{st} , the input impedance of the cochlea. A two port network model of the middle-ear can be inferred from this network model, the formulation is as follows:

$$\begin{aligned}
T_{edst11} &= \left[(Z_1 + Z_2) \cdot \frac{(Z_2 + Z_3 + Z_4)}{Z_2 \cdot Z_4} - \frac{Z_2}{Z_4} \right] & T_{edst12} &= \left[\frac{(Z_1 \cdot Z_2 + Z_1 \cdot Z_3 + Z_2 \cdot Z_3)}{Z_2} \right] \cdot 10^5 \\
T_{edst21} &= \left[\frac{(Z_2 + Z_3 + Z_4)}{Z_2 \cdot Z_4} \right] \cdot 10^5 & T_{edst22} &= \frac{(Z_2 + Z_3)}{Z_2}
\end{aligned} \tag{D.6}$$

Note that in this formulation takes into account the overall middle ear static pressure gain G_{me} (T in Kringlebotn paper), it is not included into the network picture above for simplicity. This gain is due to the influence of the area of the eardrum, of the oval window and the lever gain of the middle-ear (effective lever arm of the malleus divided by the lever arm of the incus), this is fully detailed in Kringlebotn [8]. The effect of the transformer action of the middle-ear is to improve the impedance between the source, as seen from the eardrum, and the cochlear load, and thus to increase the sound transmission to the inner ear. Also T_{edst12} and T_{edst21} are multiplied by 10^5 in order to convert these component to SI unit (Kringlebotn gives all the data in cgs units).

Inertia (g.cm ⁴)	Compliance (cm ⁴ .s ² .g ⁻¹)	Resistance (g.cm ⁴ .s ⁻²)
La=1.10 ⁻³	Ca=3.9*10 ⁻⁶	Ra=60
	Ct=0.4*10 ⁻⁶	
Ld=7.5*10 ⁻³		
Ls=66*10 ⁻³	Cs=0.3*10 ⁻⁶	Rs=20
	Cr=1.3*10 ⁻⁶	Rr=120
	Cm=0.38*10 ⁻⁶	Rm=120
Lo=22*10 ⁻³		Ro=20
	Ci=0.56*10 ⁻⁶	Ri=6000

Table 2: Parameters of the middle ear model (cgs)

D.2. Check of the reciprocity of the ear canal and middle ear models

To prove the reciprocal properties of the ear canal and middle ear models, we proceed as previously for the section of the cochlear network (see section C.3.c). For these models we observe the following relations, for a fixed frequency:

$$T_{eced11}T_{eced22} - T_{eced21}T_{eced12} = 1 \quad \text{for the ear canal} \quad (D.7)$$

and

$$T_{edst11}T_{edst22} - T_{edst21}T_{edst12} = 1 \quad \text{for the middle ear model} \quad (D.8)$$

note that the relation is observed for the middle ear model without considering the adjustment for the conversion into SI units. Consequently, these two systems are reciprocal, furthermore, considering the properties of the determinant, we have for the outer ear model (ear canal + middle-ear):

$$T_{ecst11}T_{ecst22} - T_{ecst21}T_{ecst12} = 1 \quad \text{for the outer ear model} \quad (D.9)$$

This is due to the fact that

$$\begin{bmatrix} T_{ecst11} & T_{ecst12} \\ T_{ecst21} & T_{ecst22} \end{bmatrix} = \begin{bmatrix} T_{eced11} & T_{eced12} \\ T_{eced21} & T_{eced22} \end{bmatrix} \begin{bmatrix} T_{edst11} & T_{edst12} \\ T_{edst21} & T_{edst22} \end{bmatrix} \quad (D.10)$$

D.3 Check of the reciprocity of the whole model (ear canal + middle ear + inner ear)

D.3.a. Principle

In order to test the reciprocity of the whole model (Fig.39), we proceed as follows:

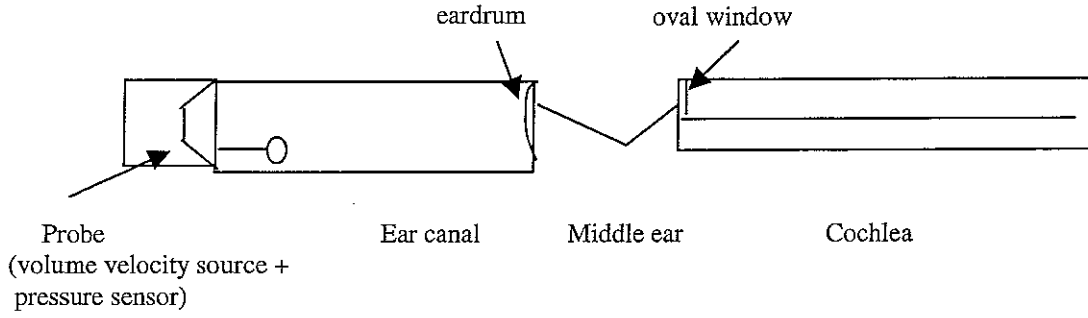


Figure 39: Representation of the whole model

In this model, the relations between the data (P_{ec} , Q_{ec}) at the entry of the ear canal and the data (P_{st} , Q_{st}) at the oval window (entry of the cochlea) are given by the two port network equation:

$$\begin{bmatrix} P_{st} \\ Q_{st} \end{bmatrix} = \begin{bmatrix} T_{11} & T_{12} \\ T_{21} & T_{22} \end{bmatrix} \begin{bmatrix} P_{ec} \\ Q_{ec} \end{bmatrix} \quad (D.11)$$

The transfer matrix being the result of the multiplication of the transfer matrices representing the ear canal and the middle ear.

To check the reciprocity of this model, we proceed in two steps:

1. First the probe imposes a volume velocity Q_0 ($\text{m}^3 \cdot \text{s}^{-1}$) (with no acoustic load) at the entry of the ear canal. The ear canal pressure and volume velocity are related to the properties of the probe by:

$$Q_{ec} = Q_0 - p_{ec} Y_0 \quad (D.12)$$

where Y_0 is the probe acoustic admittance.

If we consider the probe as a perfect volume velocity source, its admittance Y_0 can be set to zero.

$$Q_{ec} = Q_0 \quad (D.13)$$

Furthermore, to check the reciprocity, the pressure p_{ec} is set to zero. Then P_{st} and Q_{st} are obtained using equation (D.11).

$$p_{ec} = 0 \quad (D.14)$$

Then the response of the cochlea is obtained using equation (B.41), the velocity of the stapes footplate u_{st} being determined by the formula:

$$u_{st} = Q_{st} / A_{st} \quad (D.15)$$

where A_{st} is the area of the stapes footplate. Hence we can obtain the velocity of the cochlear partition and the semi difference pressure p_d at any point, at any frequency.

2. In a second step, we choose a specific point on the cochlea, referred by its index a , where we impose a disturbance S_a such as:

$$S_a = -j \omega \rho q_a \quad (\text{kg} \cdot \text{m}^{-3} \cdot \text{s}^{-2}) \quad (D.16)$$

where

$$q_a = \frac{Q_a(x, \omega)}{W * H * \Delta} \quad (D.17)$$

where Q_a is the volume velocity entailed by the motion of the basilar membrane at position x .

We modify the source array of so that we obtain exactly the same equation as (C.8). Then is computed the response of the cochlea (pressure array), the velocity of the stapes footplate (u_{st}) is obtained using the formula (B.48), and the pressure p_{st} is taken equal to $p(1)$. In order to obtain P_{ec} and Q_{ec} , we inverse the system (D.3).

Then we can compare the reports

$$Z_{ba} = \frac{P_a}{Q_{ec}} \text{ obtained with the first step and } Z_{ab} = \frac{P_{ec}}{Q_a} \text{ obtained with the second step through}$$

the third report $R: R=Z_{ab}/Z_{ba}$.

D.3.b. Results

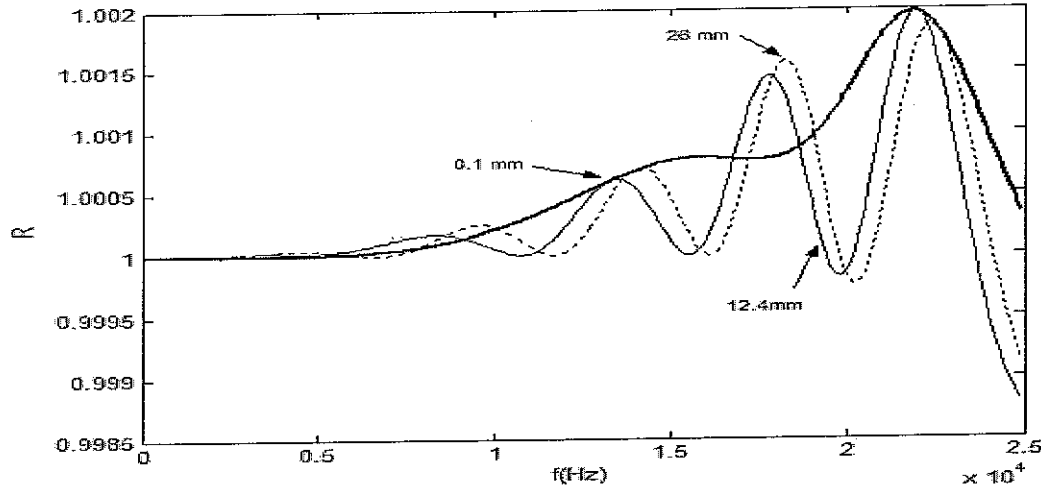


Figure 40: Reciprocity for the passive model, the point of measurement on the cochlea is at $x=0.1$ mm (bold line), $x=12.4$ mm (thin line) and $x=26$ mm (dotted line).

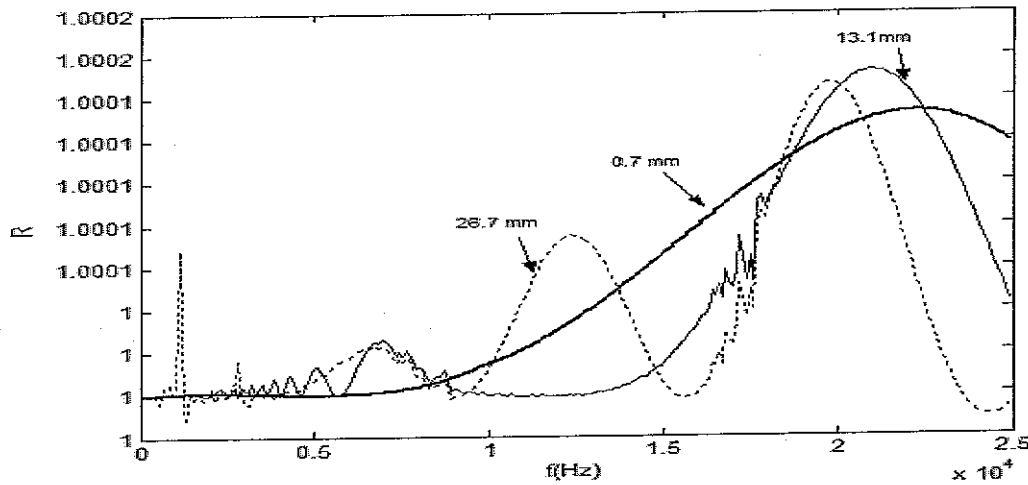


Figure 41: Reciprocity for the locally active model of Neely and Kim the point of measurement on the cochlea is at $x=0.7$ mm (bold line), $x=13.1$ mm (thin line) and $x=26.7$ mm (dotted line), active gain γ is set to 1.

Fig.40 and Fig.41 show that the ratio R is nearly equal to 1 (± 0.002), consequently it seems to be possible to consider the system as reciprocal with the conditions mentioned above. However, strong oscillations occur above 800 Hz, the source of this oscillations is not determined for the moment.

E. Stability of Neely and Kim locally active model

Note: Although it is not explicitly written, impedances Z_1 , Z_2 , Z_3 and Z_4 are dependent on both x and y , the full expressions of these quantities are given in Table 3.

E.1. Introduction

In order to simulate the high sensitivity sharp tuning characteristic of the mammalian cochlea, it is essential to include some active elements in the model. According to Neely and Kim [3], active elements are intended to represent the motile action of outer hair cells, these cells are postulated to be mechanical force generators powered by electrochemical energy of the cochlear endolymph, this electromechanical energy is controlled by the contraction of the outer hair cell stereocilia, this motion being controlled by basilar membrane motion. The model of cochlear mechanics presented in [3] is based on physical principles, anatomical characteristics and *in-vivo* response of the cochlea. In this model, the macromechanics of the cochlea are (as already mentioned previously) exactly the same as in de Boer's model, it means that a long wave model is taken for the interaction of the cochlear partition and the cochlear fluid, activity is introduced through the formulation of the cochlear partition impedance Z_{cp} . Instead of a simple spring-mass-damp model with one degree of freedom, the lumped component model of the cochlear partition is compound of two masses representing the organ of Corti (m_1) and the tectorial membrane (m_2), which displacement stand for the two degrees of freedom. A major consequence of this model is that it introduces a secondary resonance (which is tuned approximately one octave below the resonance frequency of the basilar membrane). Here is introduced the domain of micromechanics since the model we are about to describe contains structures in the organ of Corti that can move more or less independently. However, it is specifically assumed that these structures do not directly interact with the fluid. The presentation of this model is fully described in [3], it is replicated here for clarity.

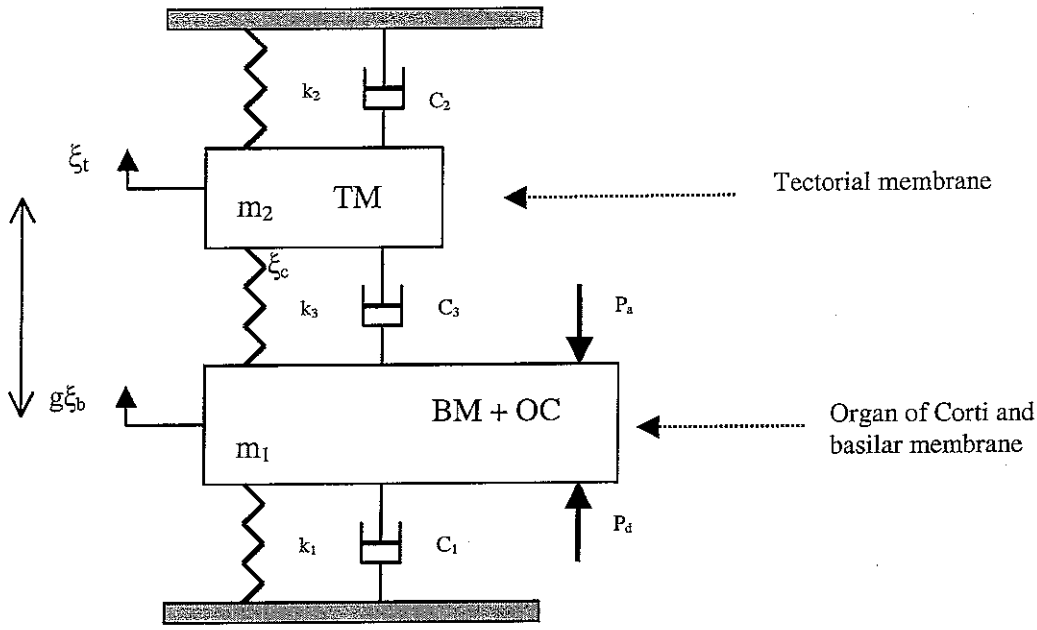


Figure 42: Lumped component of the Neely and Kim model

E.2. Description of the micromechanics

Micromechanical system proposed by Neely and Kim is reproduced on Fig.42. First, it is assumed that the cochlear partition is always displaced in the same shape (bending mode), which is independent of x . b is defined as the ratio of the average displacement across the width of the cochlear partition ξ_p to the maximum displacement over the width of the BM ξ_b , then for any given position:

$$\xi_p(x) = b\xi_b(x) \quad (\text{E.1})$$

Consequently, by this definition the value of b is always less than one.

Mechanical excitation imposed to the sensory hair cells (OHCs and IHCs) is supposed to be due to the relative shearing displacement between the tectorial membrane and the reticular lamina. ξ_c is defined to be the difference between two radially oriented displacements,

$$\xi_c(x) = g(x)\xi_b(x) - \xi_t(x) \quad (\text{E.2})$$

where $g(x)$ is the lever gain between the organ of Corti displacement ξ_b and the radial displacement of the reticular lamina and ξ_t is the radial motion of the tectorial membrane. ξ_c is used to describe the stereocilia bundle displacement of both inner and outer hair cells, at the outer hair cells it is assumed that the mechanical force generator is internal to these OHCs. At the inner hair cells it is assumed that neural rate threshold occurs at a constant peak displacement of ξ_c .

The secondary resonator consists of the tectorial membrane and the stereocilia of the outer hair cells which are partially imbedded in it. The mass originates from the tectorial

membrane and the stiffness from the stereocilia. When the basilar membrane moves, the tectorial membrane slides in a radial direction along the top membrane of the organ of Corti (reticular lamina). When the basilar moves upward, the tectorial automatically radially outward. This connection also works backwards, consequently, everything can be referred to the motion of the basilar partition.

In the model, the organ of Corti and the tectorial membrane are coupled and driven by both fluid pressure (semi difference pressure p_d) and a pressure source due to mechanical force generated by the OHC as illustrated in Fig.42. This micromechanical model has two degrees of freedom at each position x along the cochlear partition, each degree of freedom contributes a component to the radially oriented shearing displacement between the reticular lamina and the tectorial membrane. In the frequency domain, the equation of motion for the first degree of freedom (mass m_1) is:

$$p_d(x) - p_a(x) = gZ_1\dot{\xi}_b(x) + Z_3\dot{\xi}_c(x) \quad (\text{E.3})$$

where $Z_1 = i\omega m_1 + c_1 + k_1/i\omega$ and $Z_3 = c_3 + k_3/i\omega$, which represent respectively the mechanical impedance of the organ of Corti, and the coupling impedance between the organ of Corti and the tectorial membrane, and p_a is a pressure source located within the outer hair cells, this force directly acts on the basilar membrane and is capable of providing acoustical power.

The equation of motion of the second degree of freedom is:

$$Z_2\dot{\xi}_t(x) - Z_3\dot{\xi}_c(x) = 0 \quad (\text{E.4})$$

where $Z_2 = i\omega m_2 + c_2 + k_2/i\omega$ represents the mechanical impedance of the tectorial membrane.

The pressure p_a is controlled by sensory hair cell displacement ξ_c in a manner consistent with *in vitro* observations of hair cells. In vitro observation of OHCs motility shows that the height of the OHCs decreases when the cell is depolarized, this shortening of OHCs is interpreted to be the consequence of an internal pressure decrease within the OHCs. In terms of the model this means that the pressure inside the OHC decreases when the shearing displacement between the reticular lamina and the tectorial membrane (ξ_c) increases. The fluid surrounding the OHCs being assumed incompressible, internal pressure changes are transmitted isometrically to the surrounding fluid. All those observations allow Neely and Kim to define the pressure source p_a by:

$$p_a(x) = -\gamma Z_4\dot{\xi}_c(x) \quad (\text{E.5})$$

where γ is a gain factor on the active element and $Z_4 = c_4 + k_4/i\omega$ is included to provide a frequency-dependent phase shift between p_a and ξ_c . It should be noticed that γ can be regarded as a feedback coefficient.

Consequently the impedance of the cochlear partition $Z_{cp} = \frac{p_d(x)}{\dot{\xi}_p(x)}$ can be expressed as:

$$Z_{ep} = \frac{g}{b} \left[Z_1 + Z_2 \cdot \frac{(Z_3 - \gamma Z_4)}{Z_2 + Z_3} \right] \quad (\text{E.6})$$

$m_1=0.03$	$kg.m^{-2}$
$m_2=0.005$	$kg.m^{-2}$
$c_1=200+15000.e^{(-200*X)}$	$kg.m^{-2}.s^{-1}$
$c_2=100.e^{(-220*X)}$	$kg.m^{-2}.s^{-1}$
$c_3=20.e^{(-80*X)}$	$kg.m^{-2}.s^{-1}$
$c_4=10400.e^{(-200*X)}$	$kg.m^{-2}.s^{-1}$
$k_1=1.1*10^{10}.e^{(-400*X)}$	$kg.m^{-2}.s^{-2}$
$k_2=7*10^7.e^{(-440*X)}$	$kg.m^{-2}.s^{-2}$
$k_3=10^8.e^{(-400*X)}$	$kg.m^{-2}.s^{-2}$
$k_4=6.15*10^9.e^{(-400*X)}$	$kg.m^{-2}.s^{-2}$
$Z_1 = i\omega m_1 + c_1 + k_1 / i\omega$	
$Z_2 = i\omega m_2 + c_2 + k_2 / i\omega$	
$Z_3 = c_3 + k_3 / i\omega$	
$Z_4 = c_4 + k_4 / i\omega$	

Table 3: Values of the parameters of the Neely and Kim model

E.3. Build of the feedback loop system

The aim of this part is to build a feedback loop system using the equations proposed by Neely and Kim, the feedback control term being the active pressure p_a , the input term being the fluid pressure p_d and the output term being the time derivative of the shearing displacement ξ_c . The following calculation shows how this model can be formulated as a feedback control loop system.

First we have:

$$\xi_c(x) = g(x)\xi_b(x) - \xi_t(x) \quad (\text{E.7})$$

Then:

$$\dot{\xi}_c(x) = g(x)\dot{\xi}_b(x) - \dot{\xi}_t(x) \quad (\text{E.8})$$

So

$$\dot{\xi}_b(x) = \frac{\dot{\xi}_c(x) + \dot{\xi}_t(x)}{g(x)} \quad (\text{E.9})$$

Also from equation (E.4), we have:

$$\dot{\xi}_t(x) = \frac{Z_3(x).\dot{\xi}_c(x)}{Z_2(x)} \quad (\text{E.10})$$

Then

$$\dot{\xi}_b(x) = \frac{\dot{\xi}_c(x)}{g(x)} \left(1 + \frac{Z_3}{Z_2} \right) \quad (\text{E.11})$$

This expression of $\dot{\xi}_b(x)$ can be included into equation (E.3); so that we obtain:

$$p_d(x) - p_a(x) = \left(Z_1 \left(1 + \frac{Z_3}{Z_2} \right) + Z_3 \right) \dot{\xi}_c(x) \quad (\text{E.12})$$

Replacing p_a by its expression in equation (E.5),

$$p_d(x) - (-\gamma Z_4 \dot{\xi}_c) = \left(Z_1 \left(1 + \frac{Z_3}{Z_2} \right) + Z_3 \right) \dot{\xi}_c(x) \quad (\text{E.13})$$

This last equation can be written as follows

$$\underbrace{\left[\frac{1}{Z_1 \left(1 + \frac{Z_3}{Z_2} \right) + Z_3} \right]}_G p_d(x) - \underbrace{(-\gamma Z_4)}_H \underbrace{\left[\frac{1}{Z_1 \left(1 + \frac{Z_3}{Z_2} \right) + Z_3} \right]}_G \dot{\xi}_c(x) = \dot{\xi}_c(x) \quad (\text{E.14})$$

Then

$$G p_d(x) - GH \dot{\xi}_c(x) = \dot{\xi}_c(x) \quad (\text{E.15})$$

Consequently:

$$\dot{\xi}_c(x) = \frac{G}{1+GH} p_d(x) \quad (\text{E.16})$$

Thus we obtain the classical formulation for a feedback controlled system, which can be represented by the following block diagram:

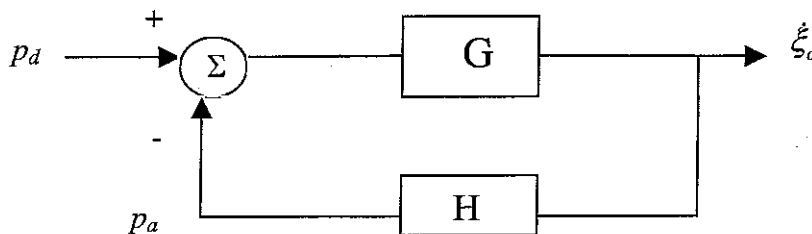


Figure 43:Block diagram of the lumped component

The stability of this system can be studied using the Nyquist criterion.

E.4. The Nyquist criterion

In this section, the stability of the single-channel continuous time controller will be discussed. The stability of a feedback system such as the one constructed above is established in terms of the positions of the poles of the closed loop transfer function. The poles of the transfer of this system is given by the roots of the characteristic equation:

$$1 + G(j\omega)H(j\omega) = 0 \quad (\text{E.17})$$

In our case, although explicit expressions for G and H are available, it remains quite tricky to extract an explicit pole/zero model of the plant G noticeably; this is mainly because the order of the plant G is quite high (4th order on the denominator after simplification of the expression of G given above). Consequently, here we consider the Nyquist definition of stability for a feedback system. The principle is to examine the polar plot of the open loop frequency response $G(j\omega)H(j\omega)$.

Provided that the plant G and the controller are themselves stable, the definition of stability supplied by the Nyquist criterion is that the polar plot of the open loop frequency response $G(j\omega)H(j\omega)$ must not enclose the point $(-1,0)$ as ω varies from $-\infty$ to $+\infty$. The locus of $G(j\omega)H(j\omega)$ for negative ω is the mirror image of the locus for positive ω about the axis since:

$$G(-j\omega)H(-j\omega) = G^*(j\omega)H^*(j\omega) \quad (\text{E.18})$$

where $*$ denotes the complex conjugation. Consequently we will limit our study of the polar plot to positive ω .

E.5 Stability of the plant G and the controller H

The stability of G and H are necessary to apply the Nyquist criterion to the whole system, to see if hidden instabilities could occur within the control loop. In our case G and H are, when isolated, passive components, they are consequently considered stable, whatever the position x on the cochlea is.

E.6. Stability of the feedback loop system

Now that the stability of G and H is ensured, we can apply the Nyquist criterion to GH , two parameters have to be considered: the influence of the position x , and the influence of the active gain γ , set by default at 1 in Neely and Kim paper [3].

Influence of the position

In this part, the active gain γ is set to 1 and Fig.44 shows the Nyquist plots for the system for $x=1, 5, 10, 15 \text{ mm}$ (left hand side) and $20, 25, 30, 35 \text{ mm}$ (right hand side);

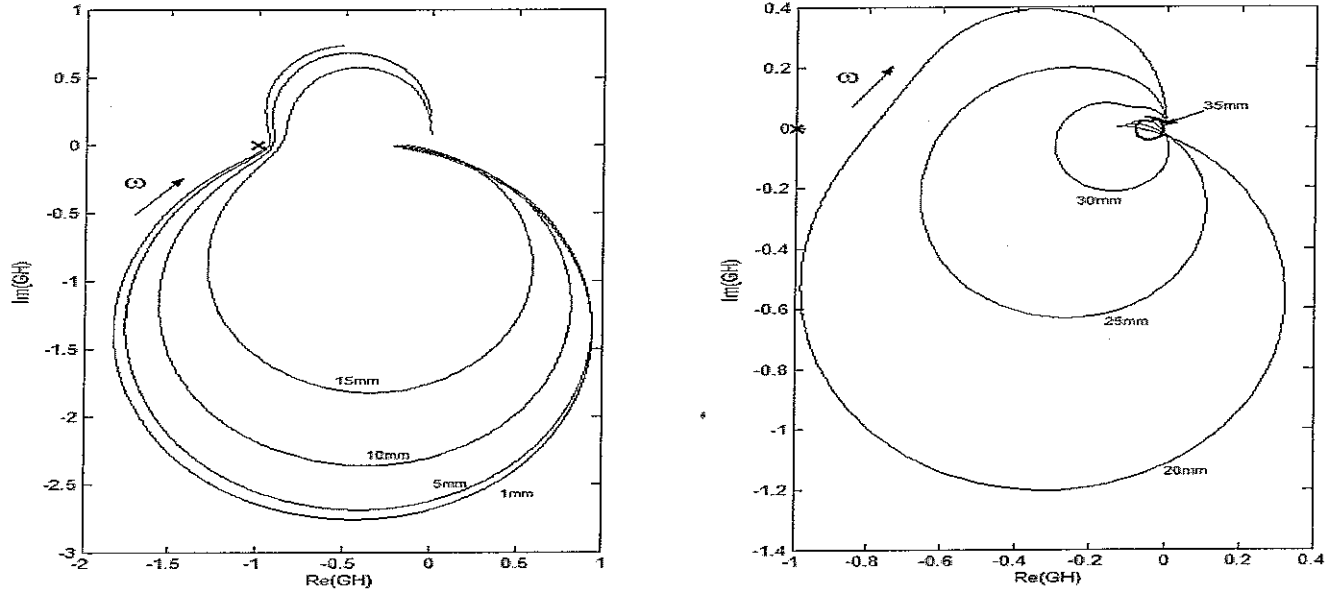


Figure 44: Nyquist plots for a fixed gain $\gamma=1$ at several positions along the cochlea from $x=1$ mm to $x=35$ mm

Fig.44 bring some comments, first it allows us to say that the lumped component of the Neelly and Kim model is more stable as it moves further from the basal end, since the Nyquist plot is further left from the point $(-1,0)$ as the position x increases. For the figures above, the active gain γ is set to 1 and stability seems to be achieved even for the components very close to the basal end, this will be checked further. Nevertheless, this stability does not seem to be extremely “robust” given that the Nyquist passes very close to the “Nyquist” point $(-1,0)$ for the components close to the basal end, we have probably very weak gain and phase margins for this system, little changes in the parameters could entail the instability of the system. The proximity of the Nyquist plots to the $(-1, 0)$ at some frequencies for small values of x indicates that the close loop gain is high, and so the cochlea is particularly active at those frequencies.

Influence of the gain γ

In this part, the influence of the gain γ is evaluated at several positions, four values for the gain are taken $\gamma=0.1$, $\gamma=0.5$, $\gamma=1$ and $\gamma=1.1$.

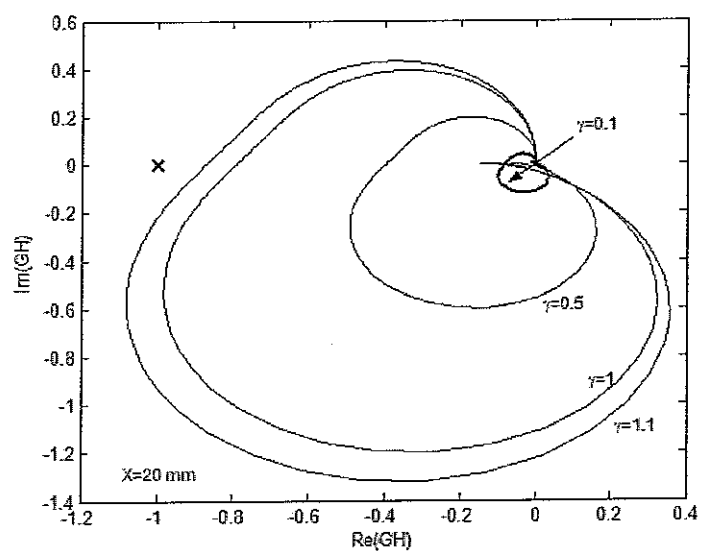
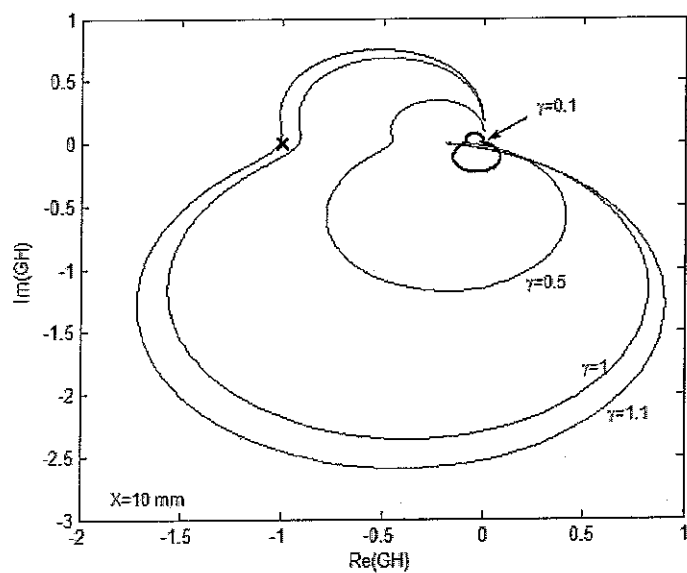
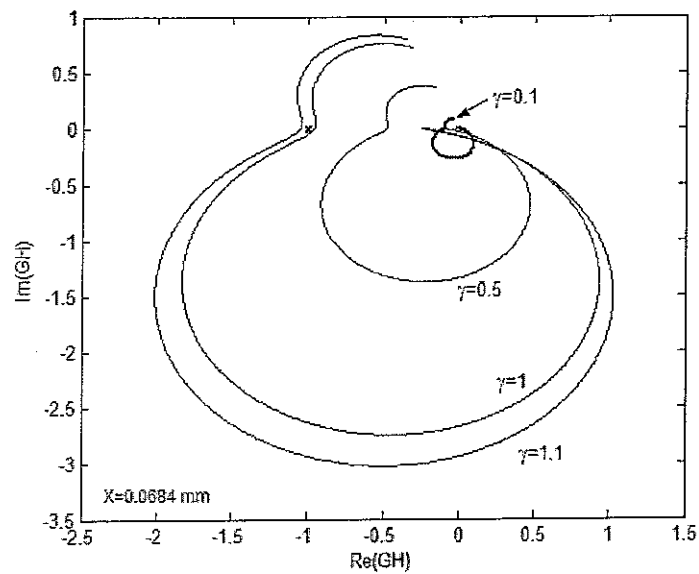


Figure 45 (a, b, c): Nyquist plots for 3 positions on the cochlea, with several gains ($\gamma=0.1, 0.5, 1, 1.1$)

As illustrated by the Fig.45, the stability of the Neely and Kim component is all the most robust as we go further from the basal end, furthermore the system is quickly unstable as the gain is increased from 1 to 1.1, at the position $x=0.0684$ mm (Fig.45a), and at the position $x=10$ mm (Fig.45b), but more stable if we go towards the apex (Fig.45c).

In conclusion, we can say that the Neely and Kim lumped component is “just” stable, and that a slight increase of the gain γ from 1 can result in instabilities in the system. In fact, the analytic Routh-Hurwitz criterion allows saying that all the lumped components along the cochlea (and noticeably near the basal end) provided that the active gain γ keeps below 1.044.

F.Stability of the multichannel system of the Neely and Kim locally active model

F.1.Introduction

In this part is presented an attempt to study the stability of the model proposed by Neely and Kim [3], in its multichannel version. We take into account several lumped component. Let's remind that no structural coupling is considered between two successive lumped components. The aim here is to create a block diagram for the study of the stability, the input being the semi-difference pressure, the output being the displacement of the basilar membrane, a feedback loop involving the active component will also be considered. Note that the stability of the cochlear system has been investigated by Koshigoe and Tubis [10], using the Hilbert transform, this method could be applied to a specific point of the cochlea; here we try to examine the stability of the whole system.

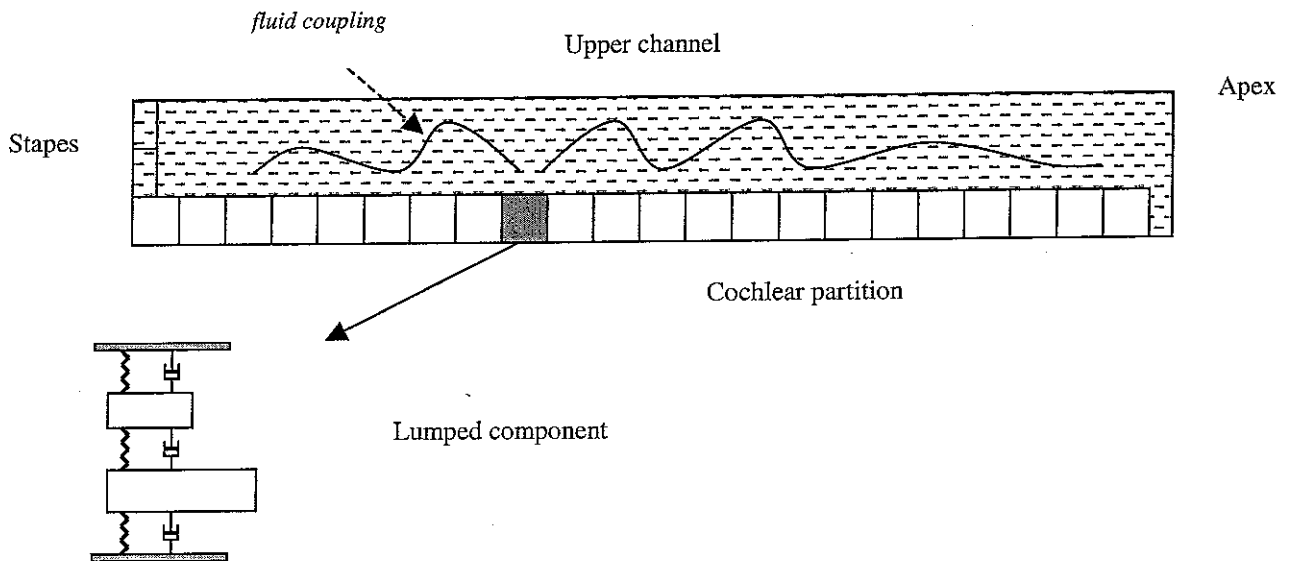


Figure 46: System considered for the study of the multichannel stability

Fig. 46 presents the system considered for the study of the stability, the cochlear partition is made up with adjacent lumped components presented in the previous section; the characteristics of the lumped component follow the relations proposed by Neely and Kim [3] in terms of mass, stiffness and damping, which are functions of the position on the cochlear partition. Given that each component is a feedback system, we can consider the system presented as a multichannel feedback system. For the study of stability, as above, we choose the Nyquist criterion applied to the eigenvalues of the system, as explained below.

F.2. Multichannel feedback control system

The aim of this part is to find a block diagram formulation adapted to the system studied. In the Neely and Kim model, at a position x the active component (pressure p_a) is dependent on the time derivative of the relative displacement ($\dot{\xi}_c$) between the two masses standing for the tectorial membrane and the organ of Corti (see section E), variations in this relative displacement are entailed by variations of the fluid pressure (p_d), the active pressure p_a is added to this fluid pressure and so on.

The extension from one to several components uses basically the same process as involved in one isolated component, noticeably for what concerns the active process, which is, for a component, not directly dependent on the behaviour of the others components in its neighbourhood. The active component is dependent on $\dot{\xi}_c(x)$, which is itself dependent on the comportment of the neighbourhood through the fluid coupling. For one component at the position x , we have:

$$p_a(x, \omega) = -\gamma Z_4(x, \omega) \cdot \dot{\xi}_c(x, \omega) \quad (\text{F.1})$$

In order to fit with our model for the study of the stability, we must exhibit the dependency of $\dot{\xi}_c(x, \omega)$ on $\dot{\xi}_b(x, \omega)$ the displacement of the basilar membrane. The approach of Neely and Kim allows us to write the following relationship between $\dot{\xi}_c(x, \omega)$ and $\dot{\xi}_b(x, \omega)$ (see section E for details):

$$\dot{\xi}_c(x, \omega) = g \left(\frac{Z_2(x, \omega)}{Z_2(x, \omega) + Z_3(x, \omega)} \right) \dot{\xi}_b(x, \omega) \quad (\text{F.2})$$

Consequently:

$$p_a(x, \omega) = -\gamma g \frac{Z_4(x, \omega) \cdot Z_2(x, \omega)}{Z_2(x, \omega) + Z_3(x, \omega)} \cdot \dot{\xi}_b(x, \omega) = -\gamma Z_H \dot{\xi}_b(x, \omega) \quad (\text{F.3})$$

$$P_a = -\gamma Z_H \cdot \Xi_b = -H \cdot \Xi_b \quad \text{for all the components} \quad (\text{F.4})$$

where \mathbf{P}_a is the array of the active component at each position $p_a(x_i)$
 \mathbf{Z}_H is the diagonal matrix of the impedance $Z_4(x_i)$ where

$$Z_H(i,i) = g \frac{Z_4(x_i, \omega) \cdot Z_2(x_i, \omega)}{Z_2(x_i, \omega) + Z_3(x_i, \omega)}$$

Ξ_b is the array where $\Xi_b(i) = \xi_b(x_i)$

$$\mathbf{H} = \gamma \mathbf{Z}_H$$

The coupling effect is here integrated into the “passive” process, the strategy to find a formulation for the passive process is to consider a totally passive system where the active part of the impedance of the lumped component is cancelled (that boils down to set $\gamma=0$), in that case the impedance Z_{pass} of the lumped component at the position x is:

$$Z_{pass} = \frac{g}{b} \left[Z_1 + Z_2 \cdot \frac{Z_3}{Z_2 + Z_3} \right] \quad (\text{F.5})$$

Consequently, the coupling process is formulated through the matrix C (as in section B.3):

$$\mathbf{C} = \frac{1}{\Delta^2} \begin{pmatrix} -\Delta & \Delta & & & & \\ 1 & -2 & 1 & & & 0 \\ & . & . & . & & \\ & & . & . & . & \\ & & & . & . & . \\ & 0 & & 1 & -2 & 1 \\ & & & & 0 & \Delta^2 \end{pmatrix} \quad (\text{F.6})$$

The mobility matrix \mathbf{M}_{pass} is, in this passive case (as in section B.3)

$$\mathbf{M}_{pass} = \frac{2j\omega\rho}{H} \begin{pmatrix} 0 & & & & & \\ & Y_{pass}(2) & & & & 0 \\ & & . & & & \\ & & & . & & \\ & & & & . & \\ 0 & & & & Y_{pass}(n-1) & \\ & & & & & 0 \end{pmatrix} \quad (\text{F.7})$$

where $Y_{pass}(i) = 1/Z_{pass}(i)$

so that we have the following passive system:

$$\mathbf{C}\mathbf{P}_d - \mathbf{M}_{\text{pass}}\mathbf{P}_d = \mathbf{S} \quad (\text{F.8})$$

where \mathbf{S} is the source term of the system its dimension is $[\text{N}^*1]$.

In order to study the stability of the system, the source S of the system is not zero, and the system is in a steady state. Actually, the source is given by the motion of the lumped components, which are motion sources for the fluid of the upper channel. The motion transmitted to the fluid is due to the motion of the basilar membrane $\xi_b(x)$ at the position x . In order to carefully formulate this source, we go back to the wave equation followed by the pressure in the fluid at the position x , which is equivalent to equation F.8:

$$\frac{\partial^2 p_d(x, \omega)}{\partial x^2} - \frac{2j\omega\rho}{HZ_{cp}(x, \omega)} p_d(x, \omega) = S(x, \omega) \quad (\text{F.9})$$

Actually, the source term can be formulated as follows

$$S(x, \omega) = -\rho \frac{\partial q}{\partial t} \quad (\text{F.10})$$

where q is a flow term which dimension is (s^{-1})

In our case, the flow term q is closely linked to $\xi_b(x)$ ($m.s^{-1}$). First we consider that the fluid motion involved by $\xi_b(x)$ is equivalent to a volume velocity injection in the upper channel. Given the dimensions of a lumped component $W*\Delta$, where W is the width of the lumped component, and of the cochlear partition, and Δ is the length of the lumped component along x direction, we can say that the volume velocity $Q_b(x)$ corresponding to this lumped component is:

$$Q_b(x, \omega) = \dot{\xi}_b(x, \omega) * W * \Delta \quad (\text{F.11})$$

Note that this motion acts *a priori* in the z -direction, nevertheless, given that motion of the fluid in the z -direction is neglected, and that the fluid is incompressible, we consider that this fluid motion is spontaneously transmitted in the x direction. Consequently the flow term generated is equivalent to:

$$q(x, \omega) = \frac{Q_b(x, \omega)}{W * H * \Delta} \quad (\text{F.12})$$

where $W*H*\Delta$ stands for the elementary volume associated to the lumped component (H being the height of the upper channel)

Thus, the flow term $q(x)$ can be written as

$$q(x, \omega) = \frac{\dot{\xi}_b(x, \omega)}{H} \quad (\text{F.13})$$

Then, the source of the wave equation is:

$$S(x, \omega) = -\frac{j\omega\rho}{H} \xi_b(x, \omega) \quad (\text{F.14})$$

At this stage, a problem appear considering the boundary conditions, indeed, the formulation of the source term $Q(x, \omega)$ is valid as long as x is different from 0 (base) and $x=L$ (apex). At the stapes we have:

$$\frac{dp_d(0)}{dx} = -j2\omega\rho u_{st} \quad (\text{F.15})$$

where u_{st} is the velocity of the stapes.

The problem is that there is no simple way to express u_{st} as a function of $\xi_c(0, \omega)$, as a result, for simplicity, we consider that there is no motion at the stapes, so that we impose a rigid boundary condition at the base of the cochlea ($u_{st}=0$), thus we can write:

$$S(0, \omega) = 0 \quad (\text{F.16})$$

At the apex, the boundary condition is

$$p_d(L) = 0 \quad (\text{F.17})$$

Consequently, we set, for conformity with the model :

$$S(L, \omega) = 0 \quad (\text{F.18})$$

The consequence of these simplifications is that in this study of stability, we only consider the motion provided by the basilar membrane itself, no external influence is considered, that is why we can say that we are studying the “internal” stability of the cochlea. A more comprehensive approach should be developed to take into account the motion of the stapes.

To sum up, according to equation F.8 and to the boundary conditions the source array \mathbf{S} can be written as follows:

$$\mathbf{S} = \begin{pmatrix} 0 & & & & \\ & B(2) & & 0 & \\ & & \ddots & & \\ & & & B(N-1) & \\ 0 & & & & 0 \end{pmatrix} \mathbf{E}_b \quad (\text{F.19})$$

where
$$B(i) = -\frac{j\omega\rho}{H} \quad (\text{F.20})$$

and i is the index standing for the position of the component.

$$\mathbf{S} = \mathbf{B}\mathbf{\Xi}_b \quad (\text{F.21})$$

Then equation (F.8) can be written as

$$(\mathbf{C} - \mathbf{M}_{\text{pass}})\mathbf{P}_d = \mathbf{B}\mathbf{\Xi}_b \quad (\text{F.22})$$

then

$$\mathbf{\Xi}_b = \mathbf{B}^{-1}(\mathbf{C} - \mathbf{M}_{\text{pass}})\mathbf{P}_d \quad (\text{F.23})$$

Note that \mathbf{B} is in theory not invertible, for the computation the zeros on the diagonal will be set to 1.0×10^{-12} .

Equation (F.4) and (F.23) permit on representing the system as a multichannel feedback system, with the following block diagram:

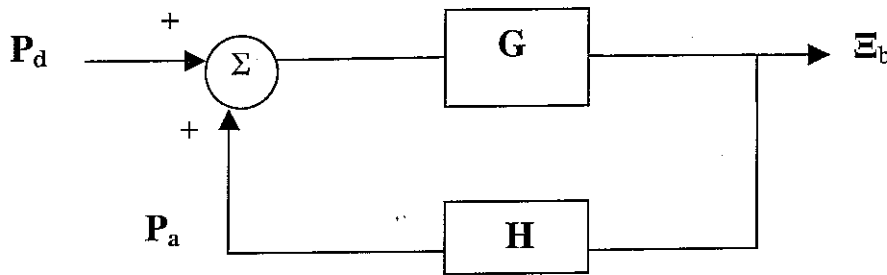


Figure 47: Block diagram representation of the multichannel feedback control system

where $\mathbf{G} = \mathbf{B}^{-1}(\mathbf{C} - \mathbf{M}_{\text{pass}})$.

F.3. Method for the study of stability, generalization of the Nyquist criterion

The stability of a multichannel feedback control system can be determined from the open-loop frequency response using a generalization of the Nyquist criterion as in Elliott [11]. As previously for the single channel system, this can be applied provided that both the plant (\mathbf{G}) and the controller (\mathbf{H}) are independently stable. The generalized Nyquist criterion states that the closed-loop system is stable on condition that the locus of the function:

$$\det[\mathbf{I} + \mathbf{GH}] \quad (\text{F.24})$$

does not enclose the origin as ω varies from $-\infty$ to $+\infty$.

But given that,

$$\det[\mathbf{I} + \mathbf{GH}] = [1 + \lambda_1][1 + \lambda_2] \dots [1 + \lambda_N] \quad (\text{F.25})$$

where λ_i are the eigenvalues of the matrix \mathbf{GH} , the locus of (F.25) does not enclose the origin provided that the locus none of the eigenvalues enclose $(-1,0)$ as ω varies from $-\infty$ to $+\infty$.

F.4. Results

The results of this investigation are studied in two ways, first we consider a basic model, made up with few lumped components (7 components here), to check the stability of a reduced model, then it is done for a larger model (512 components).

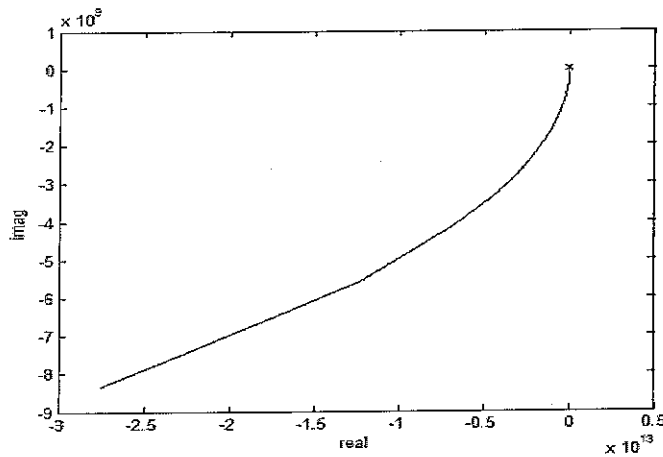


Figure 48: Evolution of the seven eigenvalues

Fig.48 is not very explicit to evaluate the evolution of the eigenvalues with frequency, in fact this figure permits to evaluate the progress of the eigenvalue associated with one of the boundary conditions. Actually, the two boundary conditions offer eigenvalues that diverge with frequency; those two eigenvalues will not be of interest further, given that they do not enclose the Nyquist point $(-1,0)$. However the eigenvalues not associated with the boundary conditions are of much interest, given that they present the same kind of evolution as the Nyquist plots for the single channel system (Fig. 49), Fig 49 corresponds to a zoom applied in Fig.50 around $(0,0)$.

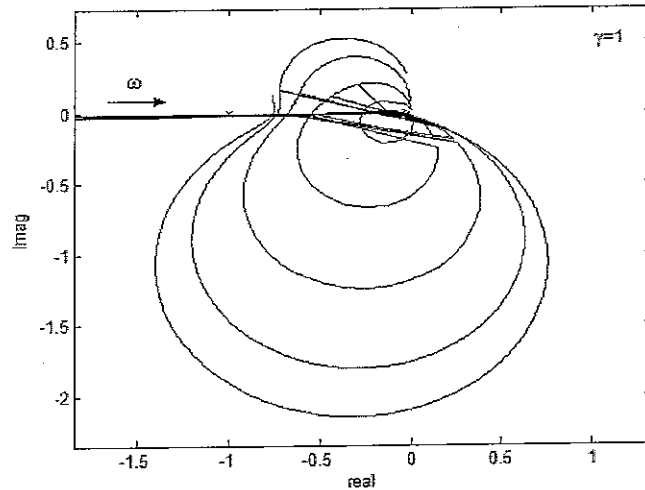


Figure 49: Evolution of the eigenvalues not associated with the boundary conditions (7 components to describe the cochlea)

Artefacts in Fig.49 are due to the fact that it has not possible to find a method to track the evolution of the eigenvalues using MATLAB, indeed EIG function makes an initial guess to find eigenvalues, but there is no way to specify this initial guess. Specifying the initial guess would not always guarantee convergence. This is one of the reasons that the EIG function does not accept an initial guess as an input argument. Nevertheless, Fig.49 allows us to see the global evolution of the eigenvalues, and to say that the locus of the 5 eigenvalues do not enclose the Nyquist point.

At this stage, it is interesting to compare these evolutions with the Nyquist plots obtained when the lumped components are considered individually.

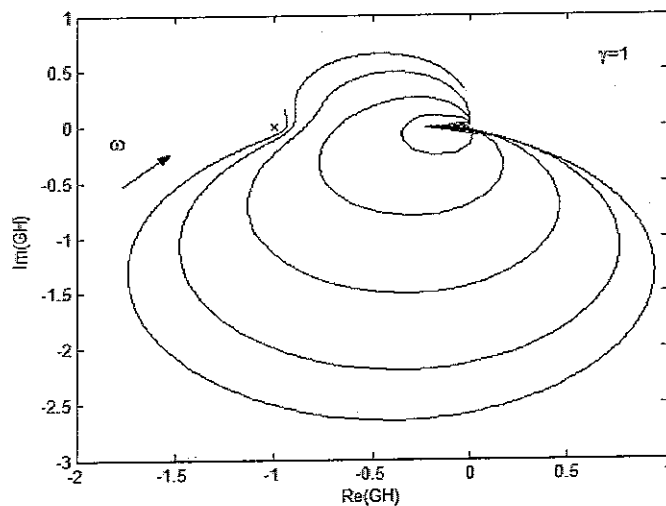


Figure 50: Evolution of the Nyquist plots when components are considered individually

Comparison between Fig.49 and Fig.50 may allow us to say that coupling between the lumped components seems to strengthen the stability of the whole model, given that the Nyquist plots keeps further from the Nyquist point in Fig.49 than in Fig.50.

If we consider 512 points to describe the cochlea in x -direction, we have roughly the same evolution as for seven points (not considering the boundary conditions once again), if we plot just 15 of these eigenvalues, we obtain:

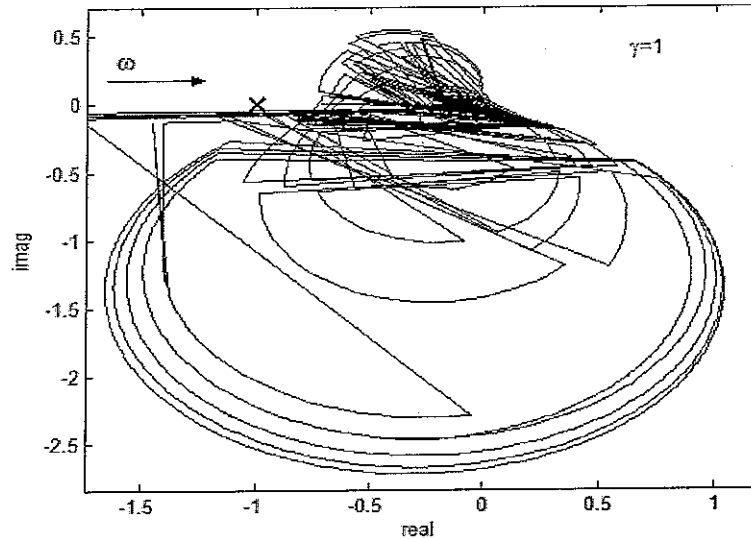


Figure 51: Nyquist plots of 15 eigenvalues from 512

Fig.51 shows that the behaviour of several eigenvalues quoted among the 512 eigenvalues is approximately comparable to what we obtain with just 7 components. (we remind once again that discrimination between these eigenvalues has not been possible using MATLAB).

To comment this brief study we can say that stability of the multichannel system seems to be checked so far; however this model for the investigation of cochlear stability still has to be improved, and most of all the formulation of the boundary conditions, and the implementation of an algorithm able to track efficiently the eigenvalues.

G. Conclusions and recommendations for future work

This work has relied on macromechanical models, the study has been conducted in the frequency domain. Three long wave models (one passive, and two locally active) are now available for further study. The validity of these models in terms of reciprocity, convergence and long-wave criterion has been checked. Now, several modifications can be brought to implement a more complete cochlear model: inhomogeneities can be introduced in the impedance of the cochlear partition as in Lineton [4], a non-linear component can also be introduced as in [2]. Even though are most often studied in the time domain, this type of model allows to implement a non-linear process.

After the computation of the model we have proposed investigations to verify the stability of the Neely and Kim locally active model, using the Nyquist plots. If we can consider that the study of stability of the lumped component is satisfactory and consistent, the study of the multichannel feedback system still needs improvements, noticeably concerning

the boundary conditions and the track of the eigenvalues, section F is, to some extent, a starting point for the study of cochlear stability in the frequency domain. Further interest on the approach proposed by Koshigoe and Tubis [10] could be relevant, but as we have already point out, this approach using the Hilbert transform can be applied only at a specific point on the cochlea, it would be interesting to try to extend this method for the investigation of the stability of the whole cochlear model. Obviously, other method for the study of the stability are available, some of them entail a time domain model (as in Diependaal et al.[12]), with most often a large computational burden.

A lot of description of the micromechanics have been proposed in the literature, Neely and Kim model is one of them. Most of these models use the same macromechanical framework as presented above, consequently the study we have done can stand for an example of procedure for the study of these kind of approaches, in terms of reciprocity and stability. Also, a comprehensive model of the ear has been developed, it can now be utilized for further work about the otoacoustic emissions for example. Also, in a future work, it would be interesting to evaluate the influence of the tapered shape of the cochlea, and why not, but the influence of the helicity of the organ.

H. References

- [1] de Boer, E. (1991) Auditory Physics. Physical principles in hearing theory III. Physics Report (Review Section of Physics Letters) 203. No.3 125-231. North-Holland
- [2] Kanis, L.J. and de Boer, E. (1993); Self-suppression in a locally active nonlinear model of the cochlea: a quasilinear approach J.Acoust.Soc.Am. 94, pp.3199-3206.
- [3] S.T. Neely, D.O. Kim (1986); A model for active element in cochlear biomechanics J.Acoust.Soc.Am. 79(5)
- [4] Lineton Benjamin (2001), Testing a Model of Stimulus Frequency Otoacoustic Emissions in Humans PhD Thesis, University of Southampton
- [5] F.J. Fahy (1995), The vibro-acoustic reciprocity principle and applications to noise control Acustica Vol.81
- [6] Kringlebotn, M (1988), Network model of the human ear Scandinavian Audiology, 17, pp.75-85.
- [7] Zweig, G and Shera, C.A. (1995) The origin of periodicity in the spectrum of evoked otoacoustic emissions J.Acoust.Soc.Am. 98, pp.2018-2047
- [8] <http://aes.cz/atp2001/proc/paper6.pdf>

- [9] Viergever, M.A., (1978). On the physical background of the point impedance characterization of the basilar membrane in cochlear mechanics, Acustica 39, 292-297
- [10] Koshigoe, K. and Tubis, A. (1982). Frequency domain investigations of cochlear stability in the presence of active elements J.Acoust.Soc.Am. 73 (4), pp.1244-1248
- [11] Elliott,S.J Signal processing for active control of sound (2000) Academic Press, Incorporated
- [12] Diependaal, R.J, Duifhuis,H., Hoogstraten,H.W., Viergever,M.A. (1987). Numerical methods for solving one-dimensional cochlear models in the time domain J.Acoust.Soc.Am. 82 (5), pp.1655-1666.
- [13] Nobili, R., Mammano, F. and Ashmore, J. (1998). How well do we understand the cochlea? TINS vol.21, No.4,1998

Figure references:

Figure 1: <http://www.homepages.ucl.ac.uk/~ucbpcjm/MResFiles/ProjectMain.pdf>

Figure 2: Pickles.J.O (1988). An introduction to the physiology of hearing (2nd ed.). London: Academic Press

Figure 3: http://media4.physics.indiana.edu/~p105_f02/Transp.html

Figure 4: <http://www.iurc.montp.inserm.fr/>

